The Canadian Mineralogist
Vol. 50, pp. 353-370 (2012)
DOI: 10.3749/canmin.50.2.353

CUPRONEYITE, $Cu_7Pb_{27}Bi_{25}S_{68}$, A NEW MINERAL SPECIES FROM BĂIŢA BIHOR, ROMANIA

GHEORGHE ILINCA[§]

Department of Mineralogy, University of Bucharest, Bd. N. Bălcescu, 1, RO–010041, Bucharest, Romania

EMIL MAKOVICKY

Department of Geology and Geophysics, University of Copenhagen, Østervoldgade 10, DK–1350 Copenhagen K, Denmark

DAN TOPA AND GEORG ZAGLER

Department of Materials Research and Physics, University of Salzburg, Hellbrunnerstrasse 34/III, A–5020, Salzburg, Austria

ABSTRACT

Cuproneyite, with an ideal formula $Cu_7Pb_{27}Bi_{25}S_{68}$, is a new mineral species found in the skarn deposit of Băiţa Bihor, Romania. The mineral occurs in irregular aggregates, nests and veinlets up to 5 cm across, with predominant cosalite, hammarite–friedrichite and calcite, within the diopside skarn. Cuproneyite is opaque, has a silver-grey color and a metallic luster, and it displays a perfect cleavage along crystal elongation. The average Mohs hardness is about 3, approximated from the average micro-identation hardness, 222.5 kg/mm^2. Cuproneyite forms irregular or short prismatic grains up to 300 μm in length, intergrown with lamellae and irregular patches of cosalite and hammarite–friedrichite. Bireflectance is barely visible in air and moderate in oil immersion, with a greyish white color and faint yellowish tints in the lightest position, to greyish white with faint bluish tints in the darkest position. Between crossed polars, the rotation tints of the most anisotropic grains are dark brownish grey to light brownish grey. Internal reflections are absent. The reflectance data (measured in air; R_{min}, R_{max}) are: 40.4, 47.1% at 470 nm, 39.3, 45.7% at 546 nm, 38.3, 44.3% at 589 nm, and 38.1, 43.9% at 650 nm. Twenty-four electron-microprobe analyses gave, as an average, Cu 3.34(12), Ag 0.30(3), Pb 40.10(27), Bi 39.59(18), Se 0.14(3), Te 0.12(4), S 16.12(7) wt%, corresponding to $Cu_{7.1}Ag_{0.38}Pb_{26.04}Bi_{25.49}(Te_{0.12}Se_{0.23}S_{67.65})_{\Sigma 68}$, calculated on the basis of (S + Se + Te) = 68 atoms per formula unit. The simplified formula [after reconversion of x(Ag + Bi) into 2xPb] is $Cu_7Pb_{27}Bi_{25}S_{68}$, in agreement with the empirical formula and the one deduced through crystal-structure analysis. Cuproneyite is monoclinic, space group $C2/m$, with a 37.432(8), b 4.0529(9), c 43.545(9) Å, β 108.800(5)°, V = 6254(2) Å^3, Z = 2, with a calculated density of 7.11 g/cm^3 . The strongest lines in the calculated X-ray powder pattern [d in Å(I)hkl] are: 3.735(96)$\overline{1}$003, 3.507(50)$\overline{3}$16, 3.464(53)$\overline{8}$011, 3.347(84)4010, 2.956(77)713, 2.925(46)$\overline{8}$014, 2.867(100)714, and 2.027(81)020. Cuproneyite is structurally related to neyite, the main difference residing in the fact that the independent Ag position present in the neyite structure is completely replaced by Cu in cuproneyite.

Keywords: cuproneyite, sulfosalt, new mineral species, crystal structure, Băiţa Bihor skarn, Romania.

INTRODUCTION

As suggested by the name, cuproneyite is chemically and structurally related to neyite, $(Cu,Ag)_2Pb_7Bi_6S_{17}$, which was discovered at Alice Arm, British Columbia, by Drummond *et al*. (1969). Neyite was distinguished by a large unit-cell: *a* 37.5, *b* 4.07, *c* 41.6 Å, β 96.8°, space group C2/*m*. Other occurrences of neyite have been described at Chishawasha, Zimbabwe (Kalbskopf & Ncube 1983), Vale das Gatas, Portugal (Gaspar & Bowles 1985), Alaska mine, Colorado (Karup-Møller & Makovicky 1992), and Benson, Arizona (Gaines *et al*. 1997). The crystal structure of neyite from Alice Arm was determined by Makovicky *et al*. (2001), where modular relationships with minerals of the junoite–felbertalite homologous series (Topa *et al*. 2000) were discussed.

The crystal structure of neyite accommodates 26 independent large cation polyhedra. The majority of these positions are mixed-occupancy positions (Pb–Bi and Pb–Bi–Ag). In addition, the structure accommodates one silver position and three copper sites (Makovicky *et al*. 2001). The Ag and Cu positions do not indicate mixed occupancies. The configuration of

§ *E-mail address*: ilinca@geo.edu.ro

the structure resembles a hypothetical third homologue of the stepped layer structure of the junoite–felbertalite homologous series (Topa *et al.* 2000), but the stacks of alternating slabs are periodically interrupted by a large $(992)_{PbS}$-like layer parallel to (001) of neyite. The central portions of the latter layer accommodate the above-mentioned site Ag1, which is fully occupied by silver.

As a result of a systematic search of the underground workings in the lower levels of the Antoniu metasomatic body at Băiţa Bihor, various samples of Bi sulfosalt mineralization were collected and analyzed by means of electron-microprobe analysis (EPMA). One of these samples, BB–06–07, was found to contain significant amounts of bismuthinite derivatives associated with cosalite and with two (Ag-poor) Bi–Pb–Cu sulfosalts containing around 3 and 5 wt% Cu, respectively, which could not be assigned to any known composition. Subsequently, a single-crystal X-ray investigation revealed that the 3 wt% Cu variety has a crystal structure closely resembling that of neyite (Makovicky *et al.* 2001), but with the Ag1 site fully occupied by Cu. Thus, in concordance with the IMA guideline on new mineral species, stating that at least one structural site in the potential new mineral should be predominantly occupied by a different chemical component than that which occurs in the equivalent site in an existing mineral species (Nickel & Grice 1998), this phase has been approved as a new mineral species, *cuproneyite* (IMA 2008–053). The type material is deposited at the Department of Mineralogy, Faculty of Geology and Geophysics, University of Bucharest, Romania (catalogue no. CATMIN 22/24).

Occurrence

Cuproneyite occurs as a result of polymetallic mineralization related to contact metamorphism developed around the Late Cretaceous magmatic complex at Băiţa Bihor, which is a part of the Banatitic Magmatic and Metallogenic Belt (BMMB: Berza *et al.*1998), which extends from the northern Apuseni Mountains, through southwestern Banat, in Romania, eastern Serbia and the Balkans (Fig. 1). Until its closure in 2008, the Băiţa Bihor mine used to be the most diverse and economically important skarn deposit in the northern Apuseni segment of the BMMB. The mine is located in the upper course of Crişul Negru River, where various lithologies belonging to the Bihor domain and Codru sedimentary nappes are intersected by numerous igneous dykes rooted in a deep granodiorite–granite pluton (Fig. 2). The Bihor domain refers to a comprehensive sedimentary cover that lies directly upon the Bihor main batholithic body and is largely affected by thermal and metasomatic metamorphism. The Codru nappes are a mixed sedimentary sequence overthrust on the Bihor domain at Băiţa Bihor along the Blidar contact and Antoniu fault (Fig. 2).

The Late Cretaceous suites are represented by a large intrusive body, composed mainly of granodiorite with subordinate granites, quartz microdiorites, syenites and various dioritic xenoliths (Stoici 1983). Numerous dykes of rhyolite, rhyodacite, dacite, andesite, basalt and lamprophyre cross-cut the entire area and form continuous outcrops extending over hundreds of meters. Dykes are 10–15 m wide and are generally oriented NW–SE, with a steep dip up to 80°.

Contact metamorphism phenomena are widespread. The vertical extent of thermal and metasomatic transformations above the roof of the main intrusive body is estimated at 1.5 km, of which more than 1000 m are well documented from drill holes. Detrital and siltic Permian rocks are transformed into hornfels of various types, such as "spotted shales" (Cioflica *et al.* 1980), varieties of aluminous hornfels with the assemblage illite – biotite – andalusite – cordierite – hematite, epidote – actinolite – tourmaline hornfels, and calc-aluminous hornfels with plagioclase – diopside – grossular (Cioflica *et al.* 1974, Stoici 1983). Peraluminous hornfels and extensive marbles formed on pure, alloclast-free carbonate rocks, add to this suite. Detailed descriptions of lithology and ore deposits are published in numerous works, *e.g.*, Cioflica *et al.* (1971, 1980, 1982), Cioflica & Vlad (1970, 1973), Ştefan *et al.* (1988), Marincea (2000), and sources quoted therein.

Skarn transformations display extremely diverse compositions and geometries, reflecting a strongly differentiated host-lithology. Proximal skarns following the magmatic contacts generally grade into complicated branching morphologies suggesting infiltration processes along pre-existing rupture zones, such as thrust planes, or networks of fractures (distal skarns). Both magmatic and postmagmatic skarns have been described (*e.g.,* Cioflica & Vlad 1970, Stoici 1983), with the latter type further divided into calcic skarns (scapolite – diopside – wollastonite – vesuvianite) and magnesian skarns (spinel – forsterite – chondrodite – phlogopite). The contact-metamorphic zone is affected by extensive boron metasomatism, especially in magnesian skarns developed at the expense of Triassic sequences of dolostones (Marincea 2000).

The mineralization is Cu- and, locally, Pb–Zn-dominated, but with a significant Mo + Bi + W + B component. It develops in calcic skarns conformable to nappe overthrusting planes or to contacts between magmatic dykes and limestones, but mostly within a series of metasomatic columns (Băiţa, Baia Roşie, Antoniu, Hoanca Moţului, Bolfu-Tony, Pregna, Frăsinel, Corlat, Coşuri, Ferdinand), *i.e.,* quasi-cylindrical structures predominantly hosted by Triassic dolomites and limestones, and extending over 400 m in depth. The columns are commonly enveloped by a thick layer of dolomitic marbles with abundant magnesian borates (kotoite, suanite, ludwigite, fluoborite, szaibélyite) grading inward to a zone with dedolomitized carbonate rocks and further to diopside – andradite – wollastonite

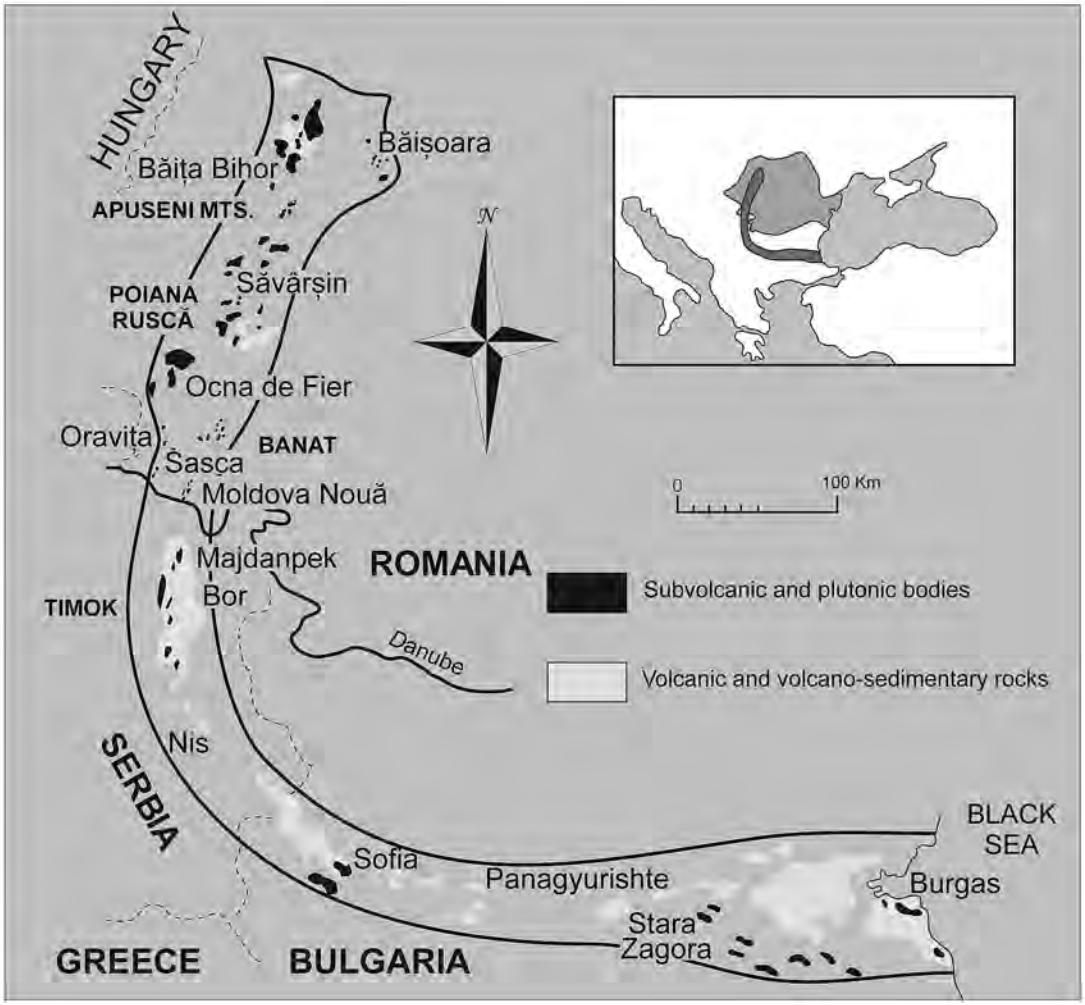

FIG. 1. The extension of the Banatitic Magmatic and Metallogenic Belt over Romania, eastern Serbia and Bulgaria (with dark grey in the inset and with heavy outline on the map). Simplified after Cioflica & Vlad (1973).

skarns. The outer shell of the skarn zone is rich in galena and sphalerite, whereas the central parts are enriched in chalcopyrite, bismuth sulfosalts, molybdenite and scheelite.

The mineralization hosting cuproneyite was intercepted by underground workings at the lower levels of the Antoniu metasomatic body, which represents a megabrecciated metasomatic column with mainly diopside (± andradite) skarns surrounded by a rim of magnesian (humite, clinochlore) skarns. Also common as gangue minerals are hydrothermal quartz, calcite and epidote. This mineralized body is developed as networks of irregular anastomosing veins up to 20 cm in diameter, nests and small concentrations of irregular shape, containing galena, sphalerite, chalcopyrite and subordinate amounts of scheelite, bismuthinite derivatives, cosalite and cuproneyite.

Recently, Băiţa Bihor has become famous for its outstanding assemblages of Bi sulfosalts. Makovickyite–cupromakovickyite exsolution textures (Topa & Paar 2008, Topa *et al.* 2008), paděraite [$Cu_{6.9}Ag_{0.2}Pb_{1.32}Bi_{11.5}S_{21.7}$], hodrušite [$Cu_{7.8}Fe_{0.3}Ag_{0.2}Bi_{11.5}S_{21.5}$], kupčikite [$Cu_{7.8}Fe_{1.1}Ag_{0.1}Bi_{10.9}Sb_{0.1}S_{21.4}$], lillianite [$Cu_{0.4}Ag_{0.9}Pb_{3.4}Bi_{5.1}Sb_{0.2}S_{11.6}$], cosalite [$Cu_{0.6}Ag_{0.4}Pb_4Bi_{4.9}S_{11.9}$], junoite [$Cu_{2.0}Ag_{0.1}Pb_{2.8}Bi_8S_{15.6}$], cannizzarite [$Cu_{0.1}Ag_{0.3}Pb_{3.7}Bi_{5.8}Sb_{0.1}S_{12.6}$], heyrovskýite [$Pb_{5.60}Ag_{0.14}Bi_{2.21}S_9$], vikingite [$Pb_{4.08}Ag_{0.16}Bi_{2.25}S_{7.5}$] (compositions from

Ilinca 1998), galenobismutite [$PbBi_2S_5$], bismuthinite derivatives (pekoite, gladite, salzburgite, paarite, krupkaite, lindströmite, emilite, hammarite, friedrichite, aikinite), emplectite [$CuBiS_2$], wittichenite [Cu_3BiS_3] and numerous tellurides and sulfotellurides emphasize the paragenetic complexities of this occurrence.

Textural Relationships Involving Cuproneyite

The mineral occurs in irregular aggregates, nests and veinlets of up to 5 cm, with predominant cosalite, within the diopside (± andradite) skarn. Under the microscope, it forms irregular or short prismatic grains, of up to 300 μm in length, intergrown with lamellae and irregular patches of cosalite and Cu–Pb-rich bismuthinite derivatives ($bd_{73–77}$, hammarite–friedrichite). Textural relations of aggregates containing cuproneyite, cosalite and hammarite–friedrichite are complex as a result of intensive replacements typical of the deposit (Fig. 3a). Cosalite seems to have been partially replaced by both phases mentioned, especially because the BSE images of cosalite suggest local Cu enrichment along contacts and planes of cleavage (Fig. 3c), as observed in the deposit of Felbertal by Topa & Makovicky (2010).

Irregular portions of selected grains of cuproneyite contain a phase darker in BSE images (Figs. 3c, d), which, after preliminary crystal-structure determination, turned out to be a variety of cuproneyite *further enriched in copper* according to a substitution scheme described below. Lengthwise sections of such aggregates reveal that the new phase replaces cuproneyite from periphery in an oriented fashion, penetrating along the 4 Å structure direction and leaving irregular to lath-like remnants of original cuproneyite in the central portions of the grains (Fig. 3d). Various shades of grey suggest that the process of substitution might locally lead to very intimate intergrowths of the two varieties of cuproneyite.

Physical Properties

The megascopic color is grey, the mineral is opaque, and the luster is metallic. The micro-indentation (VHN load: 25 g) data obtained from four indentations performed on one grain yield a mean value equal to 222.5 kg/mm^2, with the range 213–238 kg/mm^2. The Mohs hardness is 3, as approximated from VHN values. The cleavage is good, parallel to the **c** axis. No parting

FIG. 2. Geological sketch-map of Băiţa Bihor area (simplified after Stoici 1974). 1) Permian (sandstones, siltites), 2) Anisian–Norian (a: limestones, b: dolostones), 3) Lower Jurassic (shales, sandstones, black limestones), 4) Oxfordian–Tithonian (limestones, dolostones), 5) Barremian (a: limestones, b: detrital rocks), 6) Upper Cretaceous (banatites, dykes: basalts, andesites), 7) a: hornfels, b: skarns, 8) metasomatic mineralized body, 9) mining shaft, (10) cuproneyite occurrence.

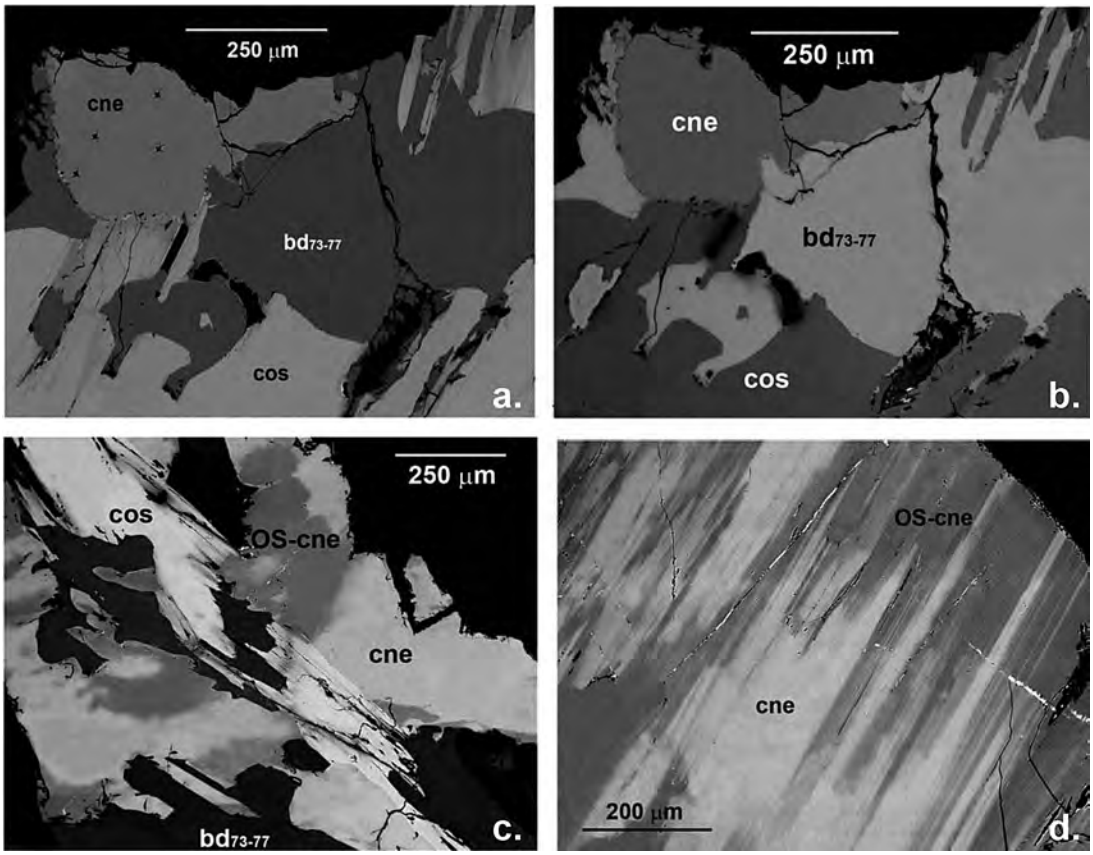

FIG. 3. Reflected-light (b) and BSE (a,c,d) images of polished fragments with a cuproneyite-containing sulfosalt assemblage. Symbols: cne: cuproneyite, OS-cne: Cu-oversubstituted cuproneyite, cos: cosalite, $bd_{73–77}$: bismuthinite–aikinite derivatives. The black areas are due to the embedding resin. The morphology of microhardness indentations is visible on the cuproneyite grain (Fig. 3a). Figure 3b showing the same assemblage as Figure 3a under cross-polarized light. Figures 3c and 3d show diffuse and epitaxic replacement relations, respectively, between cuproneyite (cne) and Cu-oversubstituted cuproneyite (OS-cne).

was observed. Cuproneyite is brittle; its fracture is subparallel, perpendicular to the **c** axis. The mineral could not be separated in a sufficiently clean fraction for direct measurements of density.

OPTICAL PROPERTIES

In plane-polarized light, the color of randomly oriented grains of cuproneyite in a polished section is greyish white (Fig. 3b). Bireflectance is perceptible in air and moderate in oil. Internal reflections are absent. Pleochroism is greyish white with faint bluish tint (darkest position) to greyish white with faint yellowish tint (lightest position). Under crossed polars, the anisotropy is moderate in air and strong in oil. Between crossed polars, the rotation tints of the most strongly anisotropic grains are dark brownish grey to light brownish grey.

Reflection data were taken using a Leitz MPV-SP microscope photometer and a WTiC as a standard. Measurement was performed in air; no measurements were made in oil. The highest R values were found at the shortest wavelengths (Table 1); the ΔR value drops with increasing wavelength as well.

CHEMICAL COMPOSITION

Cuproneyite and the associated sulfosalts minerals were analyzed using an JXA–8600 Jeol Superprobe electron microprobe, controlled by PROBE FOR WINDOWS system of programs, operated at 25 kV and 20 nA, with a beam diameter of 5 μm. Wavelength-dispersion

data were collected using the following standards (all synthetic except galena) and emission lines: Bi_2S_3 (Bi$L\alpha$, S$K\alpha$), galena (Pb$L\alpha$), chalcopyrite (Cu$K\alpha$, Fe$K\alpha$), Ag metal (Ag$L\alpha$), CdTe (Cd$L\beta$, Te$L\alpha$), and Bi_2Se_3 (Se$L\alpha$). The raw data were corrected with the on-line ZAF–4 procedure. The results of the electron-microprobe analyses are compiled in Table 2. The absence of iron, antimony, and cadmium has been noted. Tellurium and selenium are present at levels above those of the detection limits. Analytical results obtained from 24 analyses on six grains of typical cuproneyite are presented in Table 2, together with those on neyite material from other localities.

TABLE 1. REFLECTANCE DATA (IN AIR) FOR CUPRONEYITE FROM BĂIŢA BIHOR

l (nm)	R_{min} %	R_{max} %	*l* (nm)	R_{min} %	R_{max} %
400	40.21	50.25	560	38.84	45.39
420	41.61	48.13	580	38.38	44.67
440	41.29	48.12	**589**	**38.26**	**44.27**
460	40.47	47.57	600	38.20	44.46
470	**40.37**	**47.09**	620	38.04	44.18
480	40.63	47.17	640	37.84	43.76
500	40.71	47.25	**650**	**38.05**	**43.91**
520	40.18	46.63	660	37.79	43.59
540	39.48	45.85	680	37.21	43.45
546	**39.30**	**45.74**	700	37.72	43.37

Type cuproneyite has an empirical formula $Cu_{7.07}Ag_{0.38}Pb_{26.04}Bi_{25.49}S_{68}$ which, after reconversion of $x(Ag^+ + Bi^{3+})$ into $2xPb^{2+}$, gives the simplified formula $Cu_7Pb_{27}Bi_{25}S_{68}$ ($Z = 2$). High-Cu cuproneyite is further enriched in copper, as expressed by its empirical formula $Cu_{10.39}Ag_{0.40}Pb_{25.05}Bi_{25.07}S_{68}$. Chemical formulae of other known occurrences of neyite are also given in Table 2. Figure 4 shows that the chemical composition of neyite and cuproneyite can be understood in terms of "ideal unsubstituted end-members" with a definite structural site for Cu and Ag, and two substitution trends, $2Pb^{2+} = Ag^+ + Bi^{3+}$ and $Pb^{2+} = 2Cu^+$, which emanate from the "unsubstituted" compositional point. In this figure, we do not distinguish between Cu and Ag. The chemical formulae of "ideal" unsubstituted neyite and cuproneyite are contained in Table 2. Although the structural aspect of the difference between neyite and cuproneyite is clear, the structural aspect of the $Pb^{2+} = 2Cu^+$ substitution in high-Cu cuproneyite is still under study, especially because the homogeneity of this variety is an unresolved problem. With the exact

TABLE 2. AVERAGE RESULTS OF ELECTRON-MICROPROBE ANALYSES OF CUPRONEYITE, ASSOCIATED MINERALS FROM BĂIŢA BIHOR, OTHER OCCURENCES OF NEYITE, AND IDEAL END-MEMBERS

No.	mineral	*n*	Cu	Ag	Pb	Bi	Te	Se	S	Total	*ch*	*ev*	Σ*Me*	Ref.
1	cuproneyite	24	3.34(12)	0.30(03)	40.10(27)	39.59(18)	0.12(04)	0.14(03)	16.12(07)	99.71(38)	-0.01	-0.01	58.98	1
2	Cu-bearing cuproneyite	26	4.96(13)	0.32(19)	39.00(76)	39.36(40)	0.13(04)	0.11(06)	16.30(07)	100.19(58)	-0.09	-0.08	60.91	1
3	cosalite	22	1.98(07)	0.06(05)	39.04(24)	42.03(28)	0.09(05)	0.11(11)	16.21(08)	99.54(41)	-0.33	-0.30	16.59	1
4	$bd_{73.7}$	6	8.26(07)	-	27.33(17)	46.87(38)	-	0.05(04)	17.48(08)	100.16(39)	-0.50	-2.10	73.72	1
5	$bd_{77.6}$	8	8.44(15)	-	28.67(27)	44.63(37)	-	0.08(05)	17.26(16)	99.15(47)	-0.70	-2.60	77.60	1
6	neyite Dognecea	18	2.85(04)	2.17(05)	36.46(31)	41.60(20)	0.10(03)	0.09(04)	16.20(05)	99.48(38)			58.99	1
7	neyite Alice Arm	10	2.90(03)	1.58(03)	37.86(10)	40.42(13)	-	-	16.19(06)	99.29(29)	0.35	0.26	59.19	2
8	neyite Felbertal	15	2.80(03)	0.94(05)	38.89(13)	40.03(13)	-	-	16.33(10)	99.76(20)	-0.20	-0.15	58.56	3
9	unsubstituted cuproneyite		3.31	-	41.69	38.86	-	-	16.22	100				
10	Cu-enriched cuproneyite		5.26	-	38.99	39.33	-	-	16.41	100				
11	unsubstituted neyite		2.83	0.80	41.47	38.73	-	-	16.16	100				
12	Ag-bearing neyite		2.85	1.61	38.68	40.58	-	-	16.28	100				

Empirical formulae were calculated on the basis of Te + Se + S = 68 *apfu* for cuproneyite and neyite, Te + Se + S = 20 *apfu* for cosalite. Empirical formulae for bismuthinite derivatives were calculated according to the method of Makovicky & Makovicky (1978).

1) $Cu_{7.07}Ag_{0.38}Pb_{26.04}Bi_{25.49}(Te_{0.12}Se_{023}S_{67.65})_{\Sigma 68}$
2) $Cu_{10.39}Ag_{0.40}Pb_{25.05}Bi_{25.07}(Te_{0.14}Se_{0.18}S_{67.68})_{\Sigma 68}$
3) $Cu_{1.23}Ag_{0.02}Pb_{7.42}Bi_{7.92}(Te_{0.03}Se_{005}S_{19.92})_{\Sigma 20}$
4) $Cu_{2.93}Pb_{2.97}Bi_{5.05}S_{12.27}$
5) $Cu_{3.04}Pb_{3.17}Bi_{4.89}S_{12.36}$
6) $Cu_{6.02}Ag_{2.70}Pb_{23.59}Bi_{26.68}(Te_{0.10}Se_{0.16}S_{67.74})_{\Sigma 68}$
7) $Cu_{8.16}Ag_{1.97}Pb_{24.97}Bi_{26.09}S_{68}$
8) $Cu_{5.87}Ag_{1.16}Pb_{25.81}Bi_{25.72}S_{68}$
9) $Cu_7Pb_{27}Bi_{25}S_{68}$
10) $Cu_{11}Pb_{25}Bi_{25}S_{68}$
11) $Cu_6AgPb_{27}Bi_{25}S_{68}$
12) $Cu_6Ag_2Pb_{25}Bi_{26}S_{68}$

Compositions are expressed in wt.%; *n*: number of analyses. Standard deviation for the last two digits is shown in parentheses; *ch* and *ev* express the absolute and relative error in the charge balance based on the basis of cation and anion charges. References: 1) this study, 2) Makovicky *et al.* (2001), 3) D. Topa, unpublished data.

sites and possible extent of this substitution still not well constrained, it might be premature to try to define the stoichiometry of the substituted end-members.

X-Ray-Diffraction Data

For our single-crystal investigation, irregular, blade-like fragments were extracted from the polished specimen (Fig. 3a). Intensity data were collected on a Bruker AXS P3 diffractometer operated at 50 kV and 35 mA, equipped with a CCD area detector using graphite-monochromated Mo*K*α radiation. Experimental data are listed in Table 3. The SMART (Bruker AXS, 1998a) system of programs was used for unit-cell determination and data collection, SAINT+ (Bruker AXS, 1998b) for the reduction of the intensity data, and XPREP (Bruker AXS, 1997) for space-group determination and empirical absorption-correction based on pseudo-Ψ scans. The centrosymmetric space-group *C*2/*m*, proposed by the XPREP program, was chosen. It is consistent with the monoclinic symmetry of the lattice and intensity statistics (mean |E*E – 1| = 1.120 [expected values: 0.968 for the centrosymmetric case and 0.736 for the noncentrosymmetric case]). The structure of cuproneyite was solved by direct methods (program SHELXS by Sheldrick 1997a), which revealed most of the positions of the atoms. In subsequent cycles of the refinement (program SHELXL by Sheldrick 1997b), remaining atom-positions were deduced from difference-Fourier syntheses by selecting from among the strongest maxima at appropriate distances. There are 26 heavy cation (Bi and Pb) sites, four Cu sites and 34 S sites. The site-occupancy factors for all Cu sites refine to the scattering power of a Cu atom and were subsequently fixed. The site-occupancy factor of one *Me* sites (*Me*16) is significantly lower (indicating the presence of a lighter element) compared with the site-occupancy factors of the remaining ones. The small amount of Ag was placed here. In the final stage of refinement, all positions were treated as anisotropic, and the occupancy of the *Me*16 and Ag site was left free. Data on the X-ray diffraction and the structure refinement are summarized in Table 3. Positional and displacement parameters refined are given in Table 4, selected interatomic distances in Table 5, and coordination-polyhedron characteristics calculated with IVTON program (Balić-Žunić & Vicković 1996) in Table 6. Tables listing the observed and calculated structure-factors and a cif file may be obtained from the Depository of Unpublished Data on the Mineralogical Association of Canada website [document Cuproneyite CM50_353]. The site labeling and the crystal structure of cuproneyite are illustrated in Figures 5 and 6, respectively.

TABLE 3. SINGLE-CRYSTAL X-RAY DIFFRACTION OF CUPRONEYITE: EXPERIMENTAL AND REFINEMENTS DETAILS

Crystal data	
Chemical formula	$Cu_{14}AgPb_{52}Bi_{51}S_{136}$
Chemical formula weight	26789.5
Crystal system, space group	Monoclinic, *C2/m*
Cell parameters *a*, *b* (Å)	37.432(8), 4.0529(9)
Cell parameters *c* (Å), β (°)	43.545(9), 108.800(5)
Cell volume *V* (Å^3)	6254(2)
Z	1
D_x (mg m^{-3})	7.113
No. of reflections for cell parameters	5054
μ (mm^{-1})	72.95
Crystal habit	irregular
Crystal size (mm)	0.04 × 0.08 × 0.150
Crystal color	metallic dark grey
Data collection	
T_{min}, T_{max}	0.0999, 0.7488
No. of measured reflections	21616
No. of independent reflections	8278
No. of observed reflections	6050 for $F_o > 4\sigma(F_o)$
Criterion for observed reflections	$I > 2\sigma(I)$
R_{int}, R_σ (%)	11.24, 10.40
θ_{min}, θ_{max} (°)	1.39, 28.3
Range of *h*, *k*, *l*	$-50 \le h \le 39$, $-5 \le k \le 5$ $-57 \le l \le 56$
Refinement	
Refinement on F_o^2	
R_1 [$F_o > 4\sigma(F_o)$] (%)	8.08
wR (F_o^2) (%)	11.30
S (GooF)	1.062
No. of reflections used	8328
No. of parameters refined	385
Weighting scheme $w = 1/[\sigma^2(F_o^2) + (0.0916P)^2 + 361.7P]$, where $P = (F_o^2 + 2F_c^2) / 3$	
$(\Delta/\sigma)_{max}$	0.001
$\Delta\rho_{max}$ (e/Å^3)	8.48 [2.22 Å from S22]
$\Delta\rho_{min}$ (e/Å^3)	–5.94 [1.30 Å from Bi16]
Extinction coefficient	0.000006(3)
Source of scattering factors of atoms	*International Tables for Crystallography* (1992, Vol. C, Tables 4.2.6.8 and 6.1.1.4)
Computer programs	
Structure solution	*SHELXS97* (Sheldrick 1997a)
Structure refinement	*SHELXL97* (Sheldrick 1997b)

Cuproneyite is monoclinic, with *a* 37.432(8), *b* 4.0529(9), *c* 43.545(9) Å, β 108.800(5)°, *V* = 6254(2) Å^3, space group *C*2/*m*, and with *Z* = 2, for a structural formula $Cu_7Pb_{27}Bi_{25}S_{68}$. The calculated density is 7.11 g/cm^3. Its theoretical powder-diffraction pattern (Table 7) was calculated using PowderCell 2.3 software (Kraus & Nolze 1999) for a Debye–Scherrer configuration. We used Cu*K*α radiation (λ=1.540598 Å), a fixed slit, no correction for anomalous dispersion, and unit-cell parameters, space group, atom positions, site occupancy and anisotropic displacement factors from the refined structure.

Description of the Crystal Structure

Relations with the structure of neyite

Cuproneyite is an isotype of neyite. As described by Makovicky *et al.* (2001), the structure of neyite accommodates 26 independent large cation polyhedra,

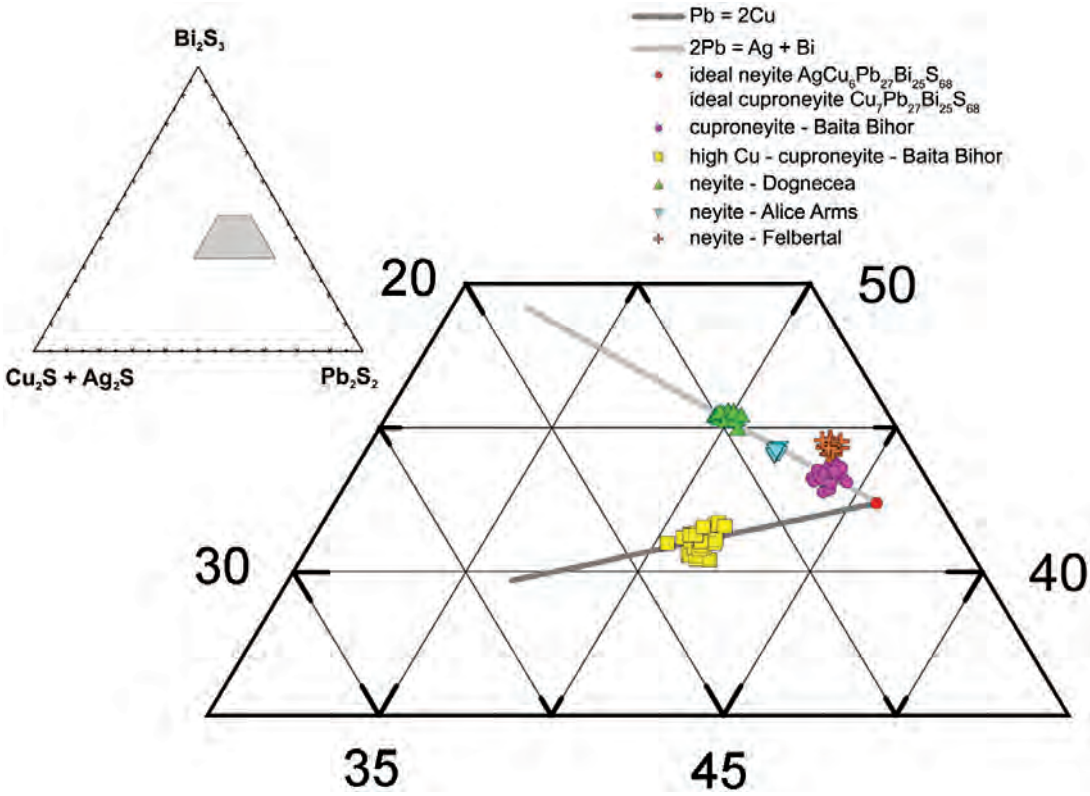

FIG. 4. Analytical data for cuproneyite and neyite varieties (at.%) in a phase diagram that does not distinguish between Ag and Cu. "Ideal" varieties have no Cu, Ag substitutions involving the coordination polyhedra of large cations, only specific Ag or Cu (or mixed) sites. Connecting lines indicate the two substitution trends, $Ag^{+} + Bi^{3+} \leftrightarrow 2Pb^{2+}$ and $2Cu^{+} \leftrightarrow Pb^{2+}$, described in the text.

one linearly coordinated silver position, three copper sites, and 34 independent sulfur sites. The majority of the large cation positions have mixed occupancies, Pb,Bi and Pb,Bi,Ag, whereas Ag and Cu positions do not indicate mixed occupancies. The structure contains $(111)_{PbS}$ slabs three octahedra thick parallel to [001] of the neyite lattice, alternating with $(100)_{PbS}$ slabs two atomic layers thick, both periodically sheared by a half-octahedron-high step. The configuration of this stacking resembles a hypothetical third homologue of the stepped layer structure of the junoite–felbertalite homologous series (Topa *et al.* 2000, 2001). The sequences of alternating slabs are periodically interrupted by a large $(992)_{PbS}$-like layer parallel to (001) of neyite. These arrangements are best illustrated by reference to Figure 6. The central part of these discordant walls accommodates a linearly coordinated Ag1site that is fully occupied by silver. Neyite has been classified as a typical sulfosalt with a "boxwork" structure (Makovicky *et al.* 2001, Moëlo *et al.* 2008, Makovicky & Topa 2009).

As a consequence, the differences with neyite are differences in the occupancy of distinct positions by cations and differences in the correspondingly adjusted bond-lengths, while preserving the topology unchanged. The unit-cell dimensions of cuproneyite are reduced compared to neyite, but only by 0.1–0.2 Å, and the angle β is not modified. The volume of the unit cell is reduced by 65 $Å^3$. The space-group symmetry is unchanged.

The defining cation position for cuproneyite, that of Cu *in linear coordination* in a flat-octahedral environment situated in the central portions of the $(001)_{ney}$ walls, displays a typical Cu–S bond length of 2.240 Å. It is to be compared with the length of the Ag–S bond for silver in this position in neyite, equal to 2.415 Å. The non-bonded distances Cu–S to the four remaining S atoms of the flat-octahedron configuration are 3.125 Å; they correspond to the Ag–S distances of the Ag octahedron in neyite, 3.139 Å. This configuration can be compared with the Cu–Se bond lengths of linearly coordinated Cu in a complex selenide, watkinsonite

TABLE 4. COORDINATES AND ANISOTROPIC DISPLACEMENT PARAMETERS OF ATOMS IN CUPRONEYITE FROM BĂIŢA BIHOR

Atom	Elem.	*x*	*z*	U_{eq}	U_{11}	U_{22}	U_{33}	U_{13}
*Me*1	Bi	0.09479(4)	0.94994(3)	0.0155(3)	0.0167(7)	0.0141(6)	0.0203(7)	0.0125(6)
*Me*2	Bi	0.43264(4)	0.13679(3)	0.0167(3)	0.0180(8)	0.0149(6)	0.0213(7)	0.0122(6)
*Me*3	m[2)]	0.31779(4)	0.07426(3)	0.0176(3)	0.0171(8)	0.0154(6)	0.0224(7)	0.0093(6)
*Me*4	m	0.20486(4)	0.01401(3)	0.0172(3)	0.0182(8)	0.0148(6)	0.0211(7)	0.0100(6)
*Me*5	m	0.04094(4)	0.77609(3)	0.0173(3)	0.0174(8)	0.0149(6)	0.0223(7)	0.0101(6)
*Me*6	m	0.15607(4)	0.83874(3)	0.0167(3)	0.0176(8)	0.0151(6)	0.0209(7)	0.0112(6)
*Me*7	m	0.27069(4)	0.90086(4)	0.0184(3)	0.0175(8)	0.0169(7)	0.0236(7)	0.0105(6)
*Me*8	Bi	0.48443(4)	0.30993(3)	0.0146(3)	0.0114(7)	0.0132(6)	0.0209(7)	0.0075(6)
*Me*9	m	0.37119(4)	0.24783(3)	0.0167(3)	0.0151(7)	0.0147(6)	0.0221(7)	0.0083(6)
*Me*10	m	0.25622(4)	0.18681(4)	0.0184(3)	0.0173(8)	0.0164(6)	0.0238(7)	0.0100(6)
*Me*11	Bi	0.09895(4)	0.66333(4)	0.0187(3)	0.0175(8)	0.0154(6)	0.0254(7)	0.0099(6)
*Me*12	Bi	0.21207(4)	0.72516(3)	0.0157(3)	0.0161(7)	0.0154(6)	0.0211(7)	0.0136(6)
*Me*13	Bi	0.40254(4)	0.52779(3)	0.0156(3)	0.0123(7)	0.0141(6)	0.0220(7)	0.0075(6)
*Me*14	Pb	0.29539(5)	0.54228(4)	0.0215(3)	0.0210(8)	0.0188(7)	0.0272(8)	0.0114(7)
*Me*15	Bi	0.18339(4)	0.53685(3)	0.0154(3)	0.0150(7)	0.0135(6)	0.0185(6)	0.0064(6)
*Me*16[1)]	Bi,Ag	0.08132(6)	0.55147(5)	0.0395(5)	0.0402(13)	0.0363(11)	0.0495(13)	0.0245(11)
*Me*17	m	0.37480(5)	0.85601(4)	0.0187(4)	0.0179(9)	0.0178(7)	0.0242(8)	0.0120(7)
*Me*18	m	0.33280(5)	0.75038(4)	0.0224(4)	0.0233(9)	0.0157(7)	0.0296(8)	0.0104(8)
*Me*19	Bi	0.31853(5)	0.65072(4)	0.0174(4)	0.0170(9)	0.0136(7)	0.0255(8)	0.0122(7)
*Me*20	Bi	0.02897(5)	0.08667(4)	0.0246(4)	0.0263(9)	0.0178(8)	0.0278(9)	0.0061(8)
*Me*21	Bi	0.06833(5)	0.19275(4)	0.0199(4)	0.0206(9)	0.0157(7)	0.0263(8)	0.0117(8)
*Me*22	Pb	0.07808(5)	0.28962(5)	0.0275(4)	0.0347(9)	0.0199(8)	0.0280(9)	0.0103(9)
*Me*23	Pb	0.10222(5)	0.38831(4)	0.0217(4)	0.0218(9)	0.0139(7)	0.0288(9)	0.0075(8)
*Me*24	Pb	0.38853(7)	0.95693(5)	0.0364(5)	0.0357(9)	0.0322(9)	0.0350(9)	0.0028(9)
*Me*25	Pb	0.00262(6)	0.41318(4)	0.0340(5)	0.0224(9)	0.0218(9)	0.0499(9)	0.0007(9)
*Me*26	Pb	0.31900(5)	0.37204(4)	0.0332(5)	0.0291(9)	0.0322(9)	0.0459(9)	0.0225(9)
Cu		0.5	0.5	0.041(3)	0.031(6)	0.064(7)	0.020(4)	-0.001(4)
Cu1		0.4689(2)	0.0104(2)	0.030(1)	0.016(3)	0.033(3)	0.041(3)	0.010(3)
Cu2		0.2314(2)	0.3094(2)	0.030(1)	0.017(3)	0.019(3)	0.057(4)	0.018(3)
Cu3		0.7494(2)	0.5896(2)	0.028(1)	0.014(3)	0.020(3)	0.0493(3)	0.008(3)
S1		0.0651(3)	-0.0042(3)	0.013(2)	0.021(4)	0.008(4)	0.020(5)	0.019(5)
S2		0.4541(3)	0.0830(3)	0.013(2)	0.003(5)	0.016(5)	0.024(5)	0.011(4)
S3		0.3522(4)	0.0181(3)	0.025(3)	0.030(7)	0.023(6)	0.023(6)	0.009(5)
S4		0.0202(3)	0.8341(3)	0.017(2)	0.010(6)	0.024(5)	0.016(5)	0.004(4)
S5		0.1281(3)	0.8935(3)	0.018(2)	0.020(6)	0.022(5)	0.016(5)	0.010(5)
S6		0.2411(4)	0.9572(3)	0.021(2)	0.027(6)	0.017(5)	0.025(6)	0.018(5)
S7		0.4916(3)	0.7453(3)	0.021(2)	0.015(6)	0.022(5)	0.029(6)	0.013(5)
S8		0.3992(4)	0.1928(3)	0.020(2)	0.026(6)	0.016(5)	0.026(5)	0.018(5)
S9		0.2875(4)	0.1283(3)	0.020(2)	0.024(6)	0.013(5)	0.028(6)	0.018(5)
S10		0.1779(3)	0.065(3)	0.022(2)	0.010(5)	0.019(5)	0.045(7)	0.021(5)
S11		0.0310(3)	0.3356(3)	0.015(2)	0.008(5)	0.008(5)	0.026(5)	0.004(5)
S12		0.0730(4)	0.7240(3)	0.022(2)	0.036(7)	0.014(5)	0.014(5)	0.006(5)
S13		0.1847(4)	0.7847(3)	0.019(2)	0.034(7)	0.010(5)	0.018(5)	0.017(5)
S14		0.2913(3)	0.8435(3)	0.027(3)	0.025(7)	0.015(5)	0.044(7)	0.018(5)
S15		0.4521(3)	0.3609(3)	0.014(2)	0.011(5)	0.016(5)	0.014(5)	0.003(4)
S16		0.3428(3)	0.3066(3)	0.020(2)	0.026(7)	0.020(5)	0.018(5)	0.012(5)
S17		0.2380(3)	0.2443(3)	0.014(2)	0.007(5)	0.011(4)	0.025(5)	0.008(4)
S18		0.0521(3)	0.4799(3)	0.020(2)	0.007(5)	0.011(5)	0.037(6)	0.002(5)
S19		0.1502(3)	0.4613(3)	0.012(2)	0.009(5)	0.010(4)	0.019(5)	0.007(4)
S20		0.2683(3)	0.4733(3)	0.014(2)	0.017(5)	0.006(4)	0.021(5)	0.011(5)
S21		0.3638(3)	0.4537(3)	0.017(2)	0.003(5)	0.016(5)	0.039(5)	0.015(5)
S22		0.4680(3)	0.4468(3)	0.021(2)	0.008(5)	0.021(5)	0.038(5)	0.011(5)
S23		0.1027(3)	0.0957(3)	0.016(2)	0.015(5)	0.016(5)	0.022(5)	0.011(5)
S24		0.1381(3)	0.1930(3)	0.017(2)	0.018(6)	0.013(5)	0.021(5)	0.008(5)
S25		0.1663(3)	0.2964(3)	0.016(2)	0.002(5)	0.022(5)	0.023(5)	0.005(5)
S26		0.1864(3)	0.3930(3)	0.019(2)	0.010(5)	0.023(5)	0.025(5)	0.008(5)
S27		0.4715(3)	0.9541(3)	0.018(2)	0.014(5)	0.021(5)	0.018(5)	0.004(5)
S28		0.4455(3)	0.8570(3)	0.020(2)	0.015(6)	0.030(6)	0.016(5)	0.009(5)
S29		0.4075(3)	0.7604(3)	0.011(2)	0.011(5)	0.013(4)	0.014(4)	0.013(4)
S30		0.3906(3)	0.6618(3)	0.014(2)	0.014(5)	0.010(4)	0.021(5)	0.011(4)
S31		0.4405(3)	0.5902(3)	0.016(2)	0.015(6)	0.015(5)	0.022(5)	0.011(5)
S32		0.2227(3)	0.5974(3)	0.014(2)	0.018(6)	0.007(4)	0.019(5)	0.010(5)
S33		0.1236(4)	0.6140(3)	0.028(2)	0.037(8)	0.024(6)	0.030(6)	0.022(6)
S34		0.2381(3)	0.6771(3)	0.016(2)	0.023(6)	0.011(4)	0.017(5)	0.013(5)

all $y = 0$, $U_{12} = 0$ and $U_{23} = 0$ by symmetry. [1)] Bi and Ag occupancy: 0.74(2) and 0.26(2). [2)] sites labeled m are mixed (Pb,Bi), with different cation proportions (see Table 6).

TABLE 5. SELECTED INTERATOMIC DISTANCES (Å) IN THE CRYSTAL STRUCTURE OF CUPRONEYITE FROM BĂIŢA BIHOR

*Me*1-		*Me*2-		*Me*3-		*Me*4-		*Me*5-		*Me*6-	
S1	2.577(11)	S2	2.706(10)	S5	2.891(07) ×2	S10	2.712(14)	S7	2.777(06) ×2	S13	2.883(11)
S2	2.798(05) ×2	S4	2.715(06) ×2	S9	2.924(11)	S6	2.845(07) ×2	S4	2.874(11)	S5	2.889(11)
S3	2.869(07) ×2	S5	3.012(07) ×2	S6	2.990(07) ×2	S3	2.944(09) ×2	S12	2.889(11)	S8	2.907(07) ×2
S5	3.102(11)	S8	3.062(16)	S3	3.109(14)	S6	3.185(16)	S8	2.999(7) ×2	S9	2.951(07) ×2
*Me*7-		*Me*8-		*Me*9-		*Me*10-		*Me*11-		*Me*12-	
S14	2.842(14)	S11	2.671(07) ×2	S12	2.888(07) ×2	S14	2.734(07) ×2	S33	2.593(16)	S34	2.583(11)
S10	2.859(07) ×2	S7	2.829(11)	S8	2.924(11)	S17	2.788(11)	S15	2.752(07) ×2	S17	2.787(06) ×2
S9	2.941(07) ×2	S15	2.839(11)	S13	2.929(07) ×2	S13	2.961(07) ×2	S16	2.962(07) ×2	S16	2.893(07) ×2
S6	2.997(11)	S12	2.974(07) ×2	S16	3.079(11)	S9	3.127(11)	S12	3.093(11)	S13	3.080(11)
*Me*13-		*Me*14-		*Me*15-		*Me*16-		*Me*17-		*Me*18-	
S31	2.625(08)	S20	2.844(08)	S32	2.578(08)	S33	2.676(12)	S28	2.634(12)	S29	2.687(11)
S18	2.738(09) ×2	S19	2.912(09) ×2	S21	2.803(09) ×2	S22	2.756(08) ×2	S23	2.845(06) ×2	S25	2.882(07) ×2
S19	2.972(09) ×2	S20	3.034(08) ×2	S20	2.844(08) ×2	S21	2.944(09)	S24	2.868(06) ×2	S24	3.103(06) ×2
S21	3.078(12)	S26	3.358(07) ×2	S19	3.111(08)	S18	2.947(09) ×2	S14	3.001(11)	S17	3.409(10) ×2
										S34	3.940(09)
*Me*19-		*Me*20-		*Me*21-		*Me*22-		*Me*23-		*Me*24-	
S30	2.581(11)	S23	2.662(11)	S24	2.625(12)	S30	2.886(06) ×2	S11	2.906(09)	S1	3.009(06) ×2
S26	2.746(06) ×2	S27	2.691(06) ×2	S29	2.810(06) ×2	S11	3.061(12)	S31	2.916(09) ×2	S10	3.110(08) ×2
S25	2.981(06) ×2	S28	3.086(06) ×2	S28	2.889(06) ×2	S29	3.146(08) ×2	S30	3.059(08) ×2	S27	3.148(12)
S34	3.550(12)	S2	3.422(07) ×2	S4	3.141(11)	S25	3.218(12)	S26	3.091(12)	S23	3.155(11) ×2
S32	3.584(09)					S7	3.267(08) ×2	S19	3.114(08)	S3	3.358(16)
*Me*25-		*Me*26-		Cu-		Cu1-		Cu2-		Cu3-	
S18	2.905(11)	S33	2.874(10) ×2	S22	2.240(12) ×2	S27	2.270(10)	S34	2.312(05) ×2	S26	2.278(12)
S31	2.980(09) ×2	S32	3.109(09) ×2	S18	3.120(10) ×4	S1	2.358(06) ×2	S25	2.313(12)	S32	2.328(07) ×2
S22	3.026(11) ×2	S34	3.202(07) ×2			S27	2.485(12)	S17	2.929(12)	S20	2.606(11)
S15	3.179(06) ×2	S16	3.240(115)			S2	3.383(11)				
S11	3.860(11)	S21	3.415(12)								

(Topa *et al*. 2010), with short bonds equal to 2.361 and 2.402 Å, and non-bonded distances equal to 3.046–3.168 Å (for closer comparison, the difference between the radii of S^{2-} and Se^{2-} should be subtracted from the Cu–Se data). Berryite (Topa *et al*. 2006) offers another linear configuration of Ag, analogous to those observed in the neyite family, with Ag–S bonds in the range 2.443–2.475 Å, and distances corresponding to non-bonded atoms, in the range 3.104–3.123 Å. The bond lengths and the occupancy refinement are consistent with an absence of Ag from the linearly coordinated site in cuproneyite.

Polyhedra and site occupancies

The adjacent octahedral site Bi16 has been partly filled by silver already in the neyite structure, where it was refined as 24% Pb, 62% Bi and 14% Ag. The site apparently accommodates the total minor Ag content found in cuproneyite; it was refined here as a single, mixed position with 76.4% Bi and 23.6% Ag. The bond lengths of the Bi16 site in cuproneyite are only slightly shorter than those of Bi16 in neyite (Makovicky *et al*. 2001).These bond lengths appear to be within a range of *Me*–S bond lengths observed for other bismuth positions in cuproneyite, which were determined, together with Bi16, as typical Bi sites in the diagram of opposing bond-lengths (Fig. 7a). The total formal positive charge of the triplet of Bi16–Cu–Bi16 sites in cuproneyite is then about +6.06, whereas in the original neyite it was calculated as +5.96, *i.e*., it can be considered unchanged.

The crystal structure of neyite displays a string of octahedral positions containing some silver in the median plane of the triple-octahedron *pseudohexagonal slab*: Bi11 (20% Ag) – Pb9 (10% Ag) – Pb6 (10% Ag); these sites are fully occupied by large cations in cuproneyite, and represent Bi or mixed (Pb,Bi) sites.

The octahedral and square-pyramidal *Me*17–*Me*21 sites belong to the pseudotetragonal Q slab, the (quasi) octahedral *Me*1–*Me*12 sites, to the pseudohexagonal triple-octahedron slab, and the *Me*13–*Me* 16 positions as well as *Me*23 and *Me*25 belong to the wall of the boxwork motif. Positions *Me*22, *Me*24, and *Me*26 have a trigonal prismatic coordination, cementing the position of different layers or slabs. The occupancy of large cation sites has been studied primarily using the hyperbolic relationship between opposing *Me*–S bonds and distances in the (quasi)octahedral configuration (Figs. 7a, b). This diagram is based on the idea of Trömmel (1981), which he applied to oxides of semimetals with a pair of lone electrons. A distinction was

made between "in-plane" and "out-of-plane" configurations, the former consisting of bonds in "square" cross-sections of octahedra ("standing" in Fig. 5), and the latter consisting of bonds to the octahedron vertices (horizontal in Fig. 5). Details of the procedure may be found in Berlepsch *et al*. (2001a, 2001b), and in a recent application, in Topa & Makovicky (2010). Points expressing the ratios of opposing bond-lengths can either fall on the hyperbola for Bi (least-squares-refined from several well-determined structures) or on that of Pb, or lie between them, expressing a mixed-cation position.

The pure Pb sites (*Me*14, 22, 23, 24, 25) are concentrated in the structure walls. Six sites (*Me*3, 4, 6, 7, 9, 10) are typical mixed positions, concentrated in the median planes and their immediate extensions in the pseudohexagonal slabs. The bismuth- or predominantly bismuth-occupied sites, with points aligned along the bismuth hyperbola, come from all three environments. Those with most asymmetric "in-plane" bonds, Bi8 and Bi20, are at the ends of their respective slabs (Fig. 6), countered only by the adjacent trigonal prisms of Pb22 and Pb24, respectively. The site of Bi20 has the most asymmetric coordination of all large cations.

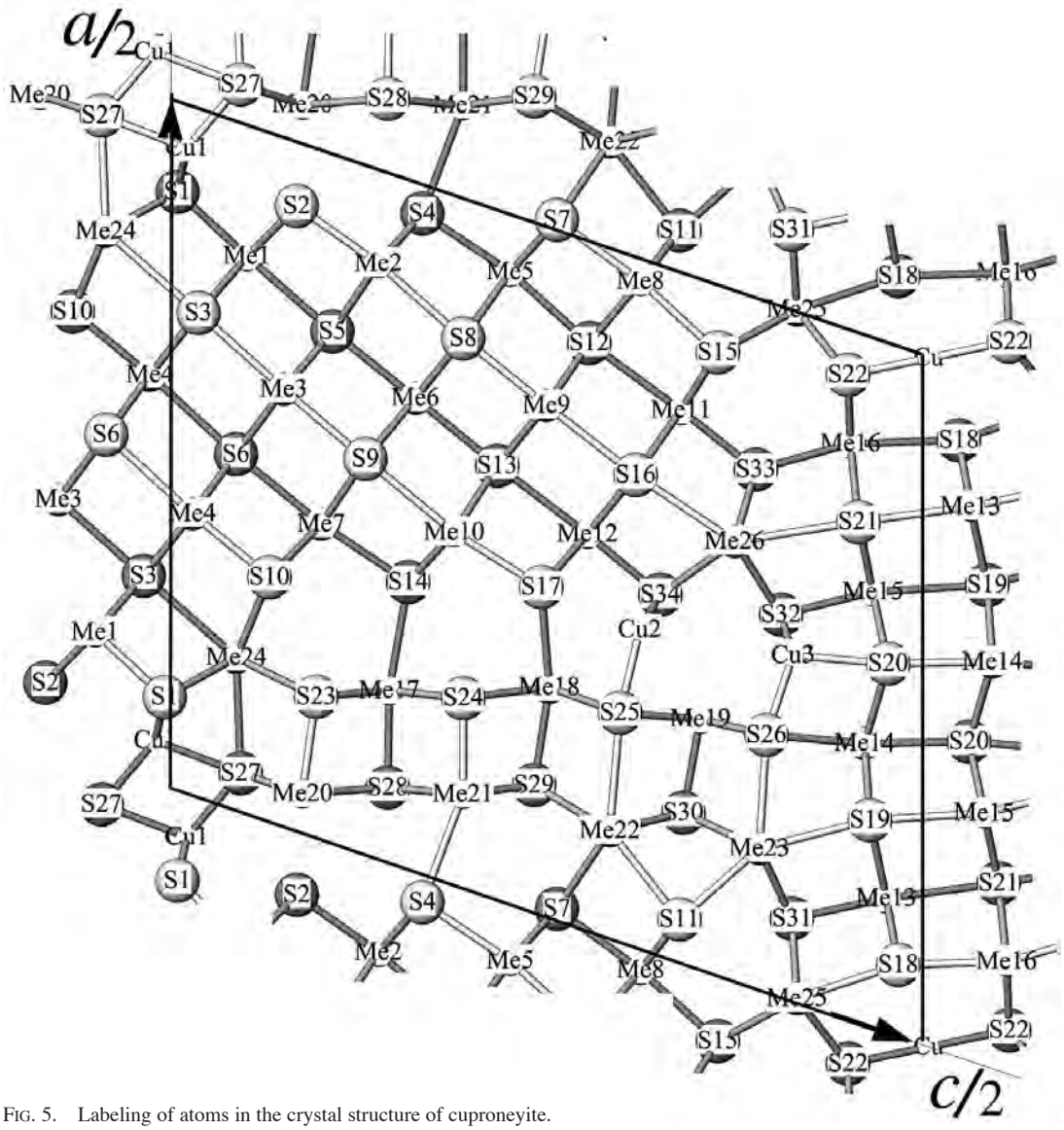

FIG. 5. Labeling of atoms in the crystal structure of cuproneyite.

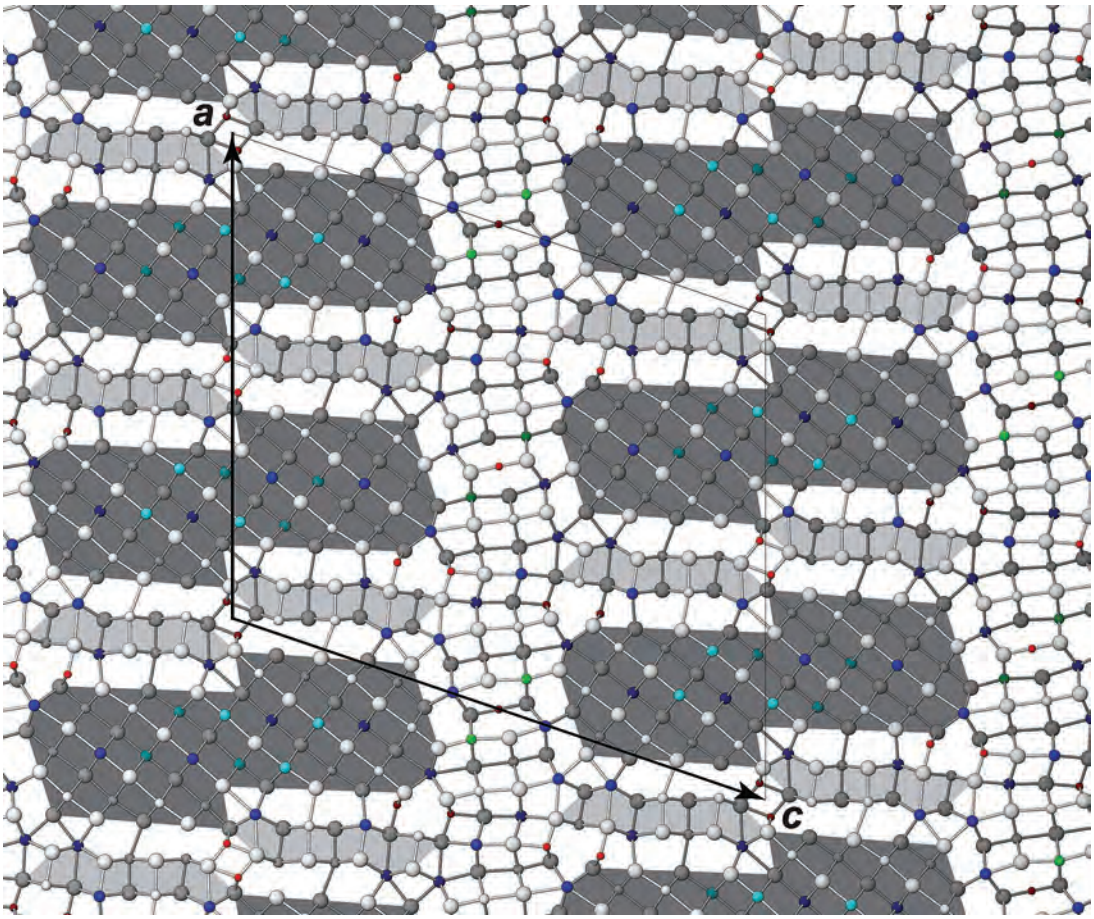

FIG. 6. The crystal structure of cuproneyite from Băiţa Bihor in projection on (010). In the order of decreasing size, the spheres (shaded according to their position on two *y* levels situated 2 Å apart) represent S sites (uncolored), Pb and Pb-dominant sites (blue), Bi and Bi-dominant sites (white), mixed-occupancy (Pb,Bi) sites (turquoise), mixed-occupancy (Bi,Ag) site (green) and Cu (red). Note the presence of three very different types of Cu sites: linear, triangular and asymmetrically tetrahedral, respectively. Shading of modules denotes: pseudohexagonal blocks $(111)_{PbS}$ in dark grey, pseudotetragonal blocks $(100)_{PbS}$ in light grey, and the large $(922)_{PbS}$ portions, parallel to (001), are left unshaded.

Most cations approximately follow their individual (mixed or pure-element) hyperbola for both the "in-plane" and "out-of-plane" configuration. Exception are the mixed-cation sites *Me*3 and *Me*9, for which the out-of-plane configuration falls onto the Pb hyperbola, and the Pb-rich *Me*18 site, with the out-of-plane data point deep in the mixed-character area. These adjustments might be the dictated by the requirements imposed by the regular arrays in which they are incorporated (*e.g.*, creating sufficient space for pairs of lone electrons of adjacent cations).

After exclusion of the mixed-character cations, there still remains a conspicuous accumulation of in-plane data points for *Me*1, 12, 15 and 21 close to the 1:1 line of the diagram; they are separated from more usual bond-length ratios represented by the field situated between *Me*16 and *Me*20. The sites Bi15 and Bi21, as well as the partly mixed *Me*17 site, are situated in a fairly symmetric environment, whereas Bi1 and Bi12 both have trigonal prismatic Pb and a copper site as neighbors. Bismuth closely associated with Cu coordination polyhedra in pavonite homologues is known to have this type of bond configuration. The other possibility is a random statistical exchange of shorter and longer in-plane bonds in one and the same coordination polyhedron, perhaps as an answer to substitutions in the adjacent polyhedra; it is well known for As, Sb and Bi (Berlepsch *et al.* 2001a, 2001b). In cuproneyite,

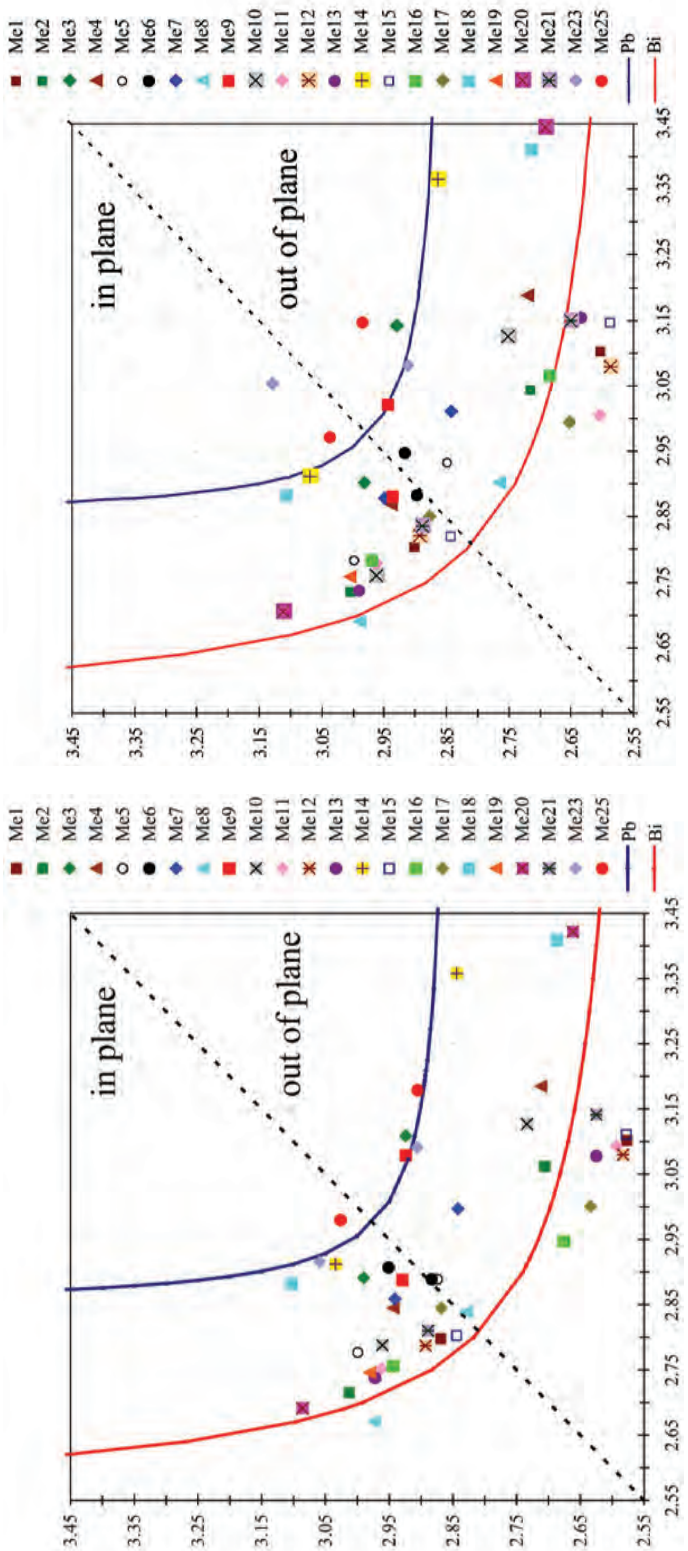

FIG. 7. Diagrams of opposing bond-lengths for octahedral and split-octahedral cation sites in the crystal structures of (a) cuproneyite and (b) neyite, respectively. In the "in-plane" octant, opposing bonds in "square" cross-sections of these coordination polyhedra ("standing" in Fig. 5) are plotted, whereas in the "out-of-plane" octant, the bonds directed toward the opposing vertices of an octahedron (horizontal bonds in Fig. 5) are displayed. Details are to be found in the text of the paper, and a detailed description of the method is provided in Berlepsch *et al.* (2001a, 2001b).

TABLE 6. POLYHEDRON CHARACTERISTICS FOR ATOMS OF CUPRONEYITE FROM BĂIŢA BIHOR

1	2	3	4	5	6	7	8	9	10	%Pb	%Bi	%Ag
*Me*1	6	2.839	0.005	0.257	0.999	95.864	30.349	3.022	Bi	13	87	0
*Me*2	6	2.865	0.001	0.260	0.987	98.466	31.323	2.761	Bi	24	76	0
*Me*3	6	2.969	0.007	0.116	0.962	109.631	34.659	1.989	m,Pb	100	0	0
*Me*4	6	2.919	0.010	0.238	0.973	104.136	32.830	2.416	m	60	40	0
*Me*5	6	2.882	0.002	0.155	0.994	100.279	31.871	2.494	m,Bi	38	62	0
*Me*6	6	2.914	0.001	0.032	0.977	103.668	32.964	2.245	m	58	32	10
*Me*7	6	2.903	0.003	0.099	0.989	102.442	32.509	2.316	m	56	44	0
*Me*8	6	2.822	0.001	0.215	0.993	94.167	29.939	3.006	Bi	0	100	0
*Me*9	6	2.942	0.004	0.084	0.953	106.668	33.803	2.124	m,Pb	69	21	10
*Me*10	6	2.877	0.001	0.229	0.940	99.775	31.727	2.611	m,Bi	33	67	0
*Me*11	6	2.856	0.008	0.282	0.990	97.623	30.826	2.936	Bi	6	74	20
*Me*12	6	2.843	0.008	0.251	0.993	96.266	30.405	2.999	Bi	10	90	0
*Me*13	6	2.864	0.013	0.269	0.999	98.358	30.900	2.899	Bi	27	73	0
*Me*14	7	3.072	0.116	0.295	0.950	121.480	40.642	1.969	Pb	100	0	0
*Me*15	6	2.838	0.014	0.258	0.995	95.708	30.025	3.060	Bi	3	97	0
*Me*16	6	2.832	0.006	0.194	0.971	95.176	30.123	2.886	Bi,Ag	24	62	14
*Me*17	6	2.854	0.023	0.177	0.970	97.424	30.305	2.840	m,Bi	6	94	0
*Me*18	8	3.163	0.047	0.442	0.812	132.606	54.806	2.174	m,Pb	100	0	0
*Me*19	7	3.014	0.108	0.480	0.897	114.697	38.710	2.849	Bi	0	100	0
*Me*20	7	3.025	0.135	0.446	0.941	115.906	37.962	2.764	Bi	0	100	0
*Me*21	6	2.881	0.065	0.249	0.999	100.154	29.823	2.810	m,Bi	0	100	0
*Me*22	8	3.112	0.033	0.183	0.912	126.207	52.909	1.910	Pb	100	0	0
*Me*23	7	3.014	0.112	0.125	0.966	114.660	38.528	2.081	Pb	100	0	0
*Me*24	8	3.136	0.037	0.062	0.905	129.221	53.947	1.710	Pb	100	0	0
*Me*25	8	3.133	0.049	0.313	0.796	128.760	53.057	1.956	Pb	100	0	0
*Me*26	8	3.128	0.037	0.091	0.836	128.180	53.529	1.869	Pb	100	0	0
Cu	6	2.826	0.057	0.001	0.518	94.583	28.393	0.849	Cu	0	0	100
Cu1	4	2.552	0.075	0.464	0.595	69.621	13.320	1.052	Cu	0	0	0
Cu2	5	2.418	0.006	0.511	1.000	59.223	7.215	0.939	Cu	0	0	0
Cu3	4	2.369	0.007	0.273	1.000	55.712	6.780	1.021	Cu	0	0	0

The polyhedron characteristics used were defined in Balić-Žunić & Makovicky (1996) and Makovicky & Balić-Žunić (1998): 1) atom label, 2) coordination number used for calculations, 3) radius r_s of a circumscribed sphere, least-squares-fitted to the coordination polyhedron, 4) volume distortion υ = [V(ideal polyhedron) – V(real polyhedron)] / V(ideal polyhedron). The ideal polyhedron has the same number of ligands. 5) "Volume-based" eccentricity $ECC_V = 1 - [(r_s - \Delta)/r_s]^3$; Δ is the distance between the center of the sphere and the central atom in the polyhedron; 6) "volume-based" sphericity $SPH_V = 1 - 3\sigma_r r_s$; σ_r is a standard deviation of the radius r_s. 7) Volume of the circumscribed sphere, 8) volume of coordination polyhedron, 9) bond-valence sum, 10) cation site-occupancy in cuproneyite suggested by the coordination and bond-valence characteristics (m: a mixed-occupancy (Pb,Bi) site. The symbols m,Pb and m,Bi indicate a mixed site with a preponderance of the indicated cation) followed by cation percentages (%Pb, *etc.*) estimated for this site in neyite by Makovicky *et al.* (2001).

these points lie close to the hyperbola (Fig. 7a), but in neyite (Fig. 7b), they appear to lie on a secant of the Bi hyperbola, which was defined as a proof of in-plane flipping of the cation position by Berlepsch *et al.* (2001a, 2001b). The only exception in neyite is Bi15, located close to Cu3. The position of these data points for cuproneyite close to the hyperbola speaks against the "flipping" hypothesis and suggests a possible trend toward a truly octahedral Bi coordination promoted by its embedding in a symmetric environment, similar to the situation in the homologues of cuprobismutite (Topa *et al.* 2003, Olsen *et al.* 2010) and in cosalite (Macíček 1986, Topa & Makovicky 2010).

Thus, the principal differences between the similar hyperbola plots for neyite and cuproneyite are (1) a larger spread of Pb values, and (2) the above-mentioned position of a number of Bi-rich points in neyite on what appears to be a secant line and not a hyperbola (Figs. 7a, b). Interestingly, in both diagrams, the out-of-plane value for *Me*6, in the interior of the H slab, almost coincides with the 1:1 line. In cuproneyite, it is joined by the points for *Me*5 and *Me*8, both tentatively positioned on the secants defined by their in-plane points. The resulting quasi-octahedral coordination might result from similar processes, as suggested in the previous paragraph.

Lead sites display larger *equivalent* atomic displacement parameters than Bi sites. The larger U_{eq} value of *Me*20 (a bismuth site) is explained by the mixed (Pb, Bi) character of the surrounding cation sites. Likewise, the augmented U_{eq} values of S3, S14 and S33 are explained in the same way.

Inspection of bond valences and polyhedron characteristics calculated by IVTON (Balić-Žunić & Vicković 1996) (Table 6) shows that they agree with the results derived from the plots of opposing bond-distances. The

polyhedron volume of octahedral Bi positions is in the range 29.9–31.3 Å^3, and that of octahedral Pb sites is about 33.8–34.6 Å^3; the mixed sites lie between these values. Seven-coordinated Bi sites have polyhedron volumes of about 38 Å^3, whereas for trigonal prismatic lead positions, the polyhedron volume is in the range 52.9–53.8 Å^3. The distortion of sites with CN greater than 6 exceeds considerably that of octahedral sites. The eccentricity of Bi is typically higher than that of Pb, but the three cation sites *Me*18–*Me*20 in the Q layers have a very high eccentricity because of their position. Bond-valence sums (Table 6) agree well with the position of cations on or between the hyperbolae of Bi and Pb. Thus, extensive substitutions, especially in the pseudohexagonal slabs, are demonstraded both by complete spectra of their bond lengths, minor statistical variations in cation positions within their polyhedra, and by the refined Z values.

The four copper sites, Cu and Cu1–3 represent three very different types of Cu coordination, linear, triangular and asymmetrically tetrahedral, respectively, all in one structure. Atom Cu2 in the interlayer space between pseudotetragonal and pseudohexagonal layers has a fairly regular triangular position. As mentioned, Cu is a linearly coordinated site inside a flattened octahedron, whereas the two remaining sites have (3 + 1) coordination in form of a distorted tetrahedral site, with one Cu–S distance substantially longer than the three Cu–S bonds (Table 5). Both tetrahedral sites are situated at the points where simple submotifs of the structure are modified or terminated, and where a "correction" to coordinates and valence is required.

Recent studies of cosalite (Topa & Makovicky 2010) revealed that the macrochemical $2Cu^{+} \leftrightarrow Pb^{2+}$ replacement may not indicate a simple exchange on the structural level, but may result from a combination of several substitutions. Therefore, it is not possible to assign the observed exchange to specific structural sites in Cu-oversubstituted cuproneyite without structural studies.

TABLE 7. CALCULATED X-RAY POWDER-DIFFRACTION DATA FOR CUPRONEYITE FROM BĂIŢA BIHOR

h	*k*	*l*	*d*, Å	*I*, rel.	*h*	*k*	*l*	*d*, Å	*I*, rel.	*h*	*k*	*l*	*d*, Å	*I*, rel.
4	0	0	8.86	6	$\bar{5}$	1	8	3.150	14	$\bar{13}$	1	14	2.0829	9
$\bar{6}$	0	3	6.20	6	1	1	8	3.118	25	$\bar{15}$	1	10	2.0729	25
$\bar{6}$	0	1	6.13	7	$\bar{8}$	0	13	3.093	7	$\bar{7}$	1	18	2.0630	7
2	0	8	4.57	6	$\bar{1}$	1	9	3.081	19	$\bar{4}$	0	21	2.0619	8
0	0	10	4.12	6	5	1	5	3.064	18	$\bar{15}$	1	11	2.0478	15
4	0	8	3.937	9	$\bar{10}$	0	12	2.9957	6	1	1	17	2.0444	20
$\bar{4}$	0	11	3.936	12	1	1	9	2.9707	14	$\bar{18}$	0	11	2.0333	7
3	1	0	3.834	11	$\bar{3}$	1	10	2.9662	18	**0**	**2**	**0**	**2.0265**	**81**
$\bar{3}$	1	3	3.797	6	**7**	**1**	**3**	**2.9557**	**77**	$\bar{1}$	1	18	2.0227	19
$\bar{10}$	**0**	**3**	**3.735**	**96**	$\bar{1}$	1	10	2.9347	7	$\bar{15}$	1	13	1.9862	6
$\bar{10}$	0	2	3.697	41	**$\bar{8}$**	**0**	**14**	**2.9249**	**46**	$\bar{4}$	0	22	1.9659	6
$\bar{10}$	0	1	3.632	15	$\bar{9}$	1	3	2.9017	29	$\bar{9}$	1	19	1.9523	9
4	0	9	3.620	16	$\bar{9}$	1	4	2.8999	11	13	1	7	1.9445	7
1	1	5	3.567	18	$\bar{9}$	1	2	2.8892	11	$\bar{5}$	1	20	1.9172	6
$\bar{5}$	1	2	3.564	8	$\bar{9}$	1	5	2.8838	24	13	1	8	1.8931	6
$\bar{5}$	1	1	3.554	21	**7**	**1**	**4**	**2.8668**	**100**	$\bar{20}$	0	5	1.8597	8
$\bar{5}$	1	3	3.547	9	$\bar{9}$	1	6	2.8543	18	17	1	0	1.8536	7
10	0	0	3.543	9	1	1	10	2.8291	11	$\bar{11}$	1	20	1.8394	12
$\bar{3}$	**1**	**6**	**3.507**	**50**	$\bar{9}$	1	7	2.8125	12	17	1	1	1.8284	19
$\bar{6}$	0	12	3.500	36	3	1	9	2.7991	8	$\bar{11}$	1	21	1.7822	9
$\bar{8}$	**0**	**11**	**3.464**	**53**	$\bar{5}$	1	11	2.7981	6	$\bar{10}$	2	3	1.7811	22
2	0	11	3.448	35	$\bar{1}$	1	11	2.7948	17	$\bar{10}$	2	2	1.7770	10
$\bar{5}$	1	5	3.441	6	9	1	2	2.7148	7	$\bar{6}$	2	12	1.7537	9
1	1	6	3.420	31	$\bar{3}$	1	12	2.7027	10	$\bar{14}$	0	23	1.7533	6
$\bar{1}$	1	7	3.382	8	9	1	3	2.6481	15	$\bar{8}$	2	11	1.7491	13
6	0	8	3.380	7	7	1	7	2.5788	6	2	2	11	1.7471	10
$\bar{3}$	1	7	3.378	64	$\bar{9}$	1	12	2.4809	9	4	2	10	1.7335	23
4	**0**	**10**	**3.347**	**84**	$\bar{13}$	1	9	2.2851	32	$\bar{6}$	2	13	1.7220	9
5	1	3	3.284	8	12	0	8	2.2662	6	11	1	14	1.7136	9
$\bar{8}$	0	12	3.273	18	9	1	8	2.2655	18	6	0	21	1.7055	12
$\bar{6}$	0	13	3.267	33	$\bar{13}$	1	10	2.2533	14	$\bar{22}$	0	7	1.6992	6
$\bar{5}$	1	7	3.259	35	12	0	9	2.1821	6	$\bar{8}$	2	14	1.6657	14
$\bar{7}$	1	2	3.226	17	1	1	16	2.1349	8	14	2	7	1.456	19
5	1	4	3.178	15	11	1	7	2.1317	15	$\bar{21}$	1	23	1.4	6
0	0	13	3.171	6	$\bar{15}$	1	4	2.1176	8	$\bar{7}$	1	30	1.365	6
7	1	0	3.164	8	$\bar{1}$	1	17	2.1117	27	21	1	11	1.307	7
$\bar{5}$	1	8	3.150	14	14	0	7	2.0934	35	6	2	21	1.305	9

Discussion

Beyond the formal aspects of mineral definition and nomenclature, the discovery of cuproneyite yields new insights into the substitutional mechanisms affecting neyite, which was originally defined as an Ag-bearing mineral. The name *cuproneyite* has been suggested to reflect this crystal-chemical relationship and to underline the end-member status of the new mineral in a potential neyite solid-solution series.

Cuproneyite is a product of an advanced stage of contact metasomatic processes, which produced an environment very rich in copper, lead and bismuth. It is especially illustrative of a "copper metasomatism" stage (CM) that affected the mineralization at Băiţa Bihor in its final phase of evolution (Ilinca 2010), and during which Bi sulfosalts were particularily sensitive to transformations resulting in copper enrichment. On the one hand, CM produced a phase in which copper assumed a role taken by silver in most other deposits. On the other hand, later metasomatic processes involving the structure of cuproneyite, with further enrichment in copper [similar to those observed for cosalite in Felbertal (Topa & Makovicky 2010), but even more pervasive] demonstrate metasomatism and element exchange of existing structures of complex sulfides, without destruction of the structure itself. The neyite–cuproneyite studies, along with those on cosalite (Topa & Makovicky 2010) and eclarite (Topa & Makovicky 2011) reveal the compositional complexity of sulfosalts, but also the strict rules of element substitutions that govern this complexity.

Dedication to my Mentor

I have no doubt saying that Emil Makovicky has exercised an overwhelming influence on the mineralogy of sulfosalts. All his scientific contributions are landmarks that are impossible to overlook, a solid foundation that we will never live to see turned into ruins. I was Emil's student some 15 years ago. I can clearly recall how he fascinated and stimulated me with his clear synoptic views over the realm of sulfosalts, with his intuitions on the regularities of this mineral group, often drafted long before physical evidence became available. I also found him mirroring a late Renaissance personality, willing and able to discover links of crystallography in any field, to discover the impact of the generalized symmetry in the most surprising places, such as decorative art, masonry or in the geometry of constructivist painting. And there was also Emil's profound humanity, his gentle, constructive and pride-disarming intransigence, that I have been praising ever since (*G. Ilinca*).

Acknowledgements

The authors gratefully acknowledge the financial support of the Christian Doppler Foundation (Austria) and the Research Council for the Nature and Universe, Denmark (grant no. 272–08–0227). Special thanks are due to Mr. D. Ardelean, without whom the cuproneyite occurrence in the deep underground works of the Băiţa Bihor mine would not have been found. Valuable comments from two anonymous reviewers and from Dr. Y. Moëlo, as well as the editorial care of Prof. R.F. Martin, have helped to improve the manuscript.

References

Balić-Žunić, T. & Makovicky, E. (1996): Determination of the centroid or 'the best centre' of a coordination polyhedron. *Acta Crystallogr.* **B52**, 78-81.

Balić-Žunić, T. & Vicković, I. (1996): IVTON – program for the calculation of geometrical aspects of crystal structures and some crystal chemical applications. *J. Appl. Crystallogr.* **29**, 305-306.

Berlepsch, P., Makovicky, E. & Balić-Žunić, T. (2001a): Crystal chemistry of meneghinite homologues and related sulfosalts. *Neues Jahrb. Mineral., Monatsh.*, 115-135.

Berlepsch, P., Makovicky, E. & Balić-Žunić, T. (2001b): Crystal chemistry of sartorite homologues and related sulfosalts. *Neues Jahrb. Mineral., Abh.* **176**, 45-66.

Berza, T., Constantinescu, E. & Vlad, Ş.N. (1998): Upper Cretaceous magmatic series and associated mineralisation in the Carpathian–Balkan orogen. *Resource Geology* **48**, 291-306.

Bruker AXS (1997): XPREP, Version 5.1, Bruker AXS, Inc., Madison,Wisconsin 53719,USA.

Bruker AXS (1998a): SMART, Version 5.0, Bruker AXS, Inc., Madison, Wisconsin 53719, USA.

Bruker AXS (1998b): SAINT, Version 5.0, Bruker AXS, Inc., Madison,Wisconsin 53719,USA.

Cioflica, G., Berbeleac, I., Lazăr, C., Ştefan, A. & Vlad, Ş.N. (1982): Metallogeny related to Laramian magmatism in the Bihor Mts. (northern Carpathians, Romania). *An. Univ. Bucureşti,* **XXXI**, 3-12.

Cioflica, G., Istrate, G., Ştefan, A. & Vlad, Ş.N. (1980): Contact metamorphism related to Laramian magmatism in Romania. Proc. XI Congress Carpathian–Balkanic Geol. Assoc., Magmatism and Metasomatism (Kiev), 204-210.

Cioflica, G. & Vlad, Ş.N. (1970): La nature polyascendante des métasomatites laramiques de Băiţa Bihorului (Monts Apuseni). *Acta Geologica Academiae Scientiarum Hungaricae* **14**, 135-141.

CIOFLICA, G. & VLAD, Ş.N. (1973): The correlation of the Laramian metallogenic events belonging to the Carpatho-Balkan area. *Rev. Roum. Géol. Géophys. Géogr.* (*sér. Géol.*) **17**, 217-214.

CIOFLICA, G., VLAD, Ş.N. & STOICI, S. (1971): Répartition de la minéralisation dans les skarns de Băiţa Bihorului. *Rev. Roum. Géol. Géophys. Géogr.* (*sér. Géol.*) **15**, 43-58.

CIOFLICA, G., VLAD, Ş.N., IOSOF, V. & PANICAN, A. (1974): Thermal and metasomatic metamorphism of Paleozoic formations in the Arieşeni unit at Băiţa Bihorului. *St. Cerc. Geol., Geof., Geog.* (*sér. Geol.*) **19**, 43–68 (in Romanian).

DRUMMOND, A.D., TROTTER, J., THOMPSON, R.M. & GOWER, J.A. (1969): Neyite, a new sulphosalt from Alice Arm, British Columbia. *Can. Mineral.* **10**, 90-96.

GAINES, R.V., SKINNER, H.C.W., FOORD, E.E., MASON, B. & ROSENZWEIG, A. (1997): *Dana's New Mineralogy*. John Wiley & Sons, Inc., New York, N.Y.

GASPAR, O. & BOWLES, J.F.W. (1985): Nota preliminar sobre a paragenete dos sulfossais de Bi–Pb–Ag do jazigo de tungstenio de Vale das Gatas, norte de Portugal. *Estudos, Notas e Trabalhos de Servico de Fomento Mineiro* (*Portugal*) **27**, 49-54.

ILINCA, G. (1998): *Crystal Chemistry of Bismuth Sulphosalts Related to Upper Cretaceous Magmatism in Romania*. Ph.D. thesis, University of Bucharest, Bucharest, Romania (in Romanian).

ILINCA, G. (2010): Classic skarn localities in Romania: contact metamorphism and mineralization related to Late Cretaceous magmatism. *Acta Mineralogica-Petrographica, Field Guide Ser., IMA2010 Field Trip Guide RO5*, **23**.

KALBSKOPF, S. & NCUBE, S.M.N. (1983): Bismuth mineralization at the Golconda prospect, Chishawasha. *Annals Zimbabwe Geol. Surv.* **9**, 135-141.

KARUP-MØLLER, S. & MAKOVICKY, E. (1992): Mummeite – a new member of the pavonite homologous series from Alaska mine, Colorado. *Neues Jahrb. Mineral., Monatsh.*, 555-576.

KRAUS, W. & NOLZE, G. (1999): POWDERCELL 2.3. Federal Institute for Materials Research and Testing, Berlin, Germany.

MACÍČEK, J. (1986): The crystal chemistry of cosalite. *Coll. Abstr. Xth Eur. Crystallogr. Meeting* (*Wroclaw*), 260.

MAKOVICKY, E. & BALIĆ-ŽUNIĆ, T. (1998): New measure of distortion for coordination polyhedra. *Acta Crystallogr.* **B54**, 766-773.

MAKOVICKY, E., BALIĆ-ŽUNIĆ, T. & TOPA, D. (2001): The crystal structure of neyite, $Ag_2Cu_6Pb_{25}Bi_{26}S_{68}$. *Can. Mineral.* **39**, 1365-1376.

MAKOVICKY, E. & MAKOVICKY, M. (1978): Representation of compositions in the bismuthinite–aikinite series. *Can. Mineral.* **16**, 405-409.

MAKOVICKY, E. & TOPA, D. (2009): The crystal structures of sulfosalts with the boxwork architecture and their new representative, $Pb_{15-2x}Sb_{14+2x}S_{36}O_x$. *Can. Mineral.* **47**, 3-24.

MARINCEA, Ş. (2000): Fluoborite in magnesian skarns from Băiţa Bihor (Bihor Massif, Apuseni Mountains, Romania). *Neues Jahrb. Mineral., Monatsh.,* 357-371.

MOËLO, Y., MAKOVICKY, E., MOZGOVA, N.N., JAMBOR, J.L., COOK, N., PRING, A., PAAR, W.H., NICKEL, E.H., GRAESER, S., KARUP-MØLLER, S., BALIĆ-ŽUNIĆ, T., MUMME, W.G., VURRO, F., TOPA, D., BINDI, L., BENTE, K. & SHIMIZU, M. (2008): Sulfosalt systematics: a review. Report of the sulfosalt sub-committee of the IMA Commission on Ore Mineralogy. *Eur. J. Mineral.* **20**, 7-46.

NICKEL, E.H. & GRICE J.D. (1998): The IMA Commission on New Minerals and Mineral Names: procedures and guidelines on mineral nomenclature, 1998. *Can. Mineral.* **36**, 913-926.

OLSEN, L.A., LÓPEZ-SOLANO, J., GARCÍA, A., BALIĆ-ŽUNIĆ, T. & MAKOVICKY, E. (2010): Dependence of the lone pair of bismuth on coordination environment and pressure: an *ab initio* study on $Cu_4Bi_5S_{10}$ and Bi_2S_3. *J. Solid State Chem.* **183**, 2133-2143.

SHELDRICK, G.M. (1997a): SHELXS-97. A Computer Program for Crystal Structure Determination. University of Göttingen, Göttingen, Germany.

SHELDRICK, G.M. (1997b): SHELXL-97. A Computer Program for Crystal Structure Refinement. University of Göttingen, Göttingen, Germany.

ŞTEFAN, A., LAZĂR, C., BERBELEAC, I. & UDUBAŞA, G. (1988): Evolution of the banatitic magmatism in the Apuseni Mts. and associated metallogenesis. *D.S. Inst. Geol. Geof.* **72–73**, 195-213.

STOICI, S.D. (1974): Geological and petrographical study of the upper course of Crisul Negru Basin – Băiţa Bihor, with special view on the boron mineralization and magnesian skarns. *St. Tehn. Ec. I.G.G.*, I/7 (in Romanian).

STOICI, S.D. (1983): *The Metallogenic District of Băiţa Bihorului*. Editura Academiei, Bucharest, Romania (in Romanian).

TOPA, D. & MAKOVICKY, E. (2010): The crystal chemistry of cosalite based on new electron-microprobe data and single-crystal determinations of the structure. *Can. Mineral.* **48**, 1081-1107.

TOPA, D. & MAKOVICKY, E. (2012): Eclarite, new data and interpretations. *Can. Mineral.* **50**, 371-386.

TOPA, D., MAKOVICKY, E. & BALIĆ-ŽUNIĆ, T. (2003): Crystal structures and crystal chemistry of members of the cuprobismutite homologous series of sulfosalts. *Can. Mineral.* **41,** 1481-1501.

TOPA D., MAKOVICKY E. & BALIĆ-ŽUNIĆ, T. (2008): What is the reason of the doubled unit cell volumes of copper–lead rich pavonite homologues? The crystal structures of cupromakovickyite and makovickyite. *Can. Mineral.* **46**, 515-523.

TOPA, D., MAKOVICKY, E., BALIĆ-ŽUNIĆ, T. & BERLEPSCH, P. (2000): The crystal structure of $Cu_2Pb_6Bi_8S_{19}$. *Eur. J. Mineral.* **12**, 825-833.

TOPA, D., MAKOVICKY, E., CRIDDLE, A., PAAR, W.H. & BALIĆ-ŽUNIĆ, T. (2001): Felbertalite, $Cu_2Pb_6Bi_8S_{19}$, a new mineral species from Felbertal, Salzburg Province, Austria. *Eur. J. Mineral.* **13**, 961-972.

TOPA, D., MAKOVICKY, E., PUTZ, H. & MUMME, W.G. (2006): The crystal structure of berryite, $Cu_3Ag_2Pb_3Bi_7S_{16}$. *Can. Mineral.* **44**, 465-480.

TOPA, D., MAKOVICKY, E., SEJKORA, J. & DITTRICH, H. (2010): The crystal structure of watkinsonite, $Cu_2PbBi_4Se_8$, from the Zálesí uranium deposit, Czech Republic. *Can. Mineral.* **48,** 1109-1118.

TOPA, D. & PAAR, W.H. (2008): Cupromakovickyite, $Cu_8Pb_4Ag_2Bi_{18}S_{36}$, a new mineral of the pavonite homologous series. *Can. Mineral.* **46**, 503-514.

TRÖMMEL, M. (1981): Abstandskorrelationen bei der Tellur(IV)-Sauerstoff- und bei der Antimon(III)-Sauerstoff-Koordination. *Z. Kristallogr.* **154**, 338-339.

Received March 17, 2011, revised manuscript accepted February 25, 2012.

```
data_cuproneyite

_audit_creation_method            SHELXL-97
_chemical_name_systematic
;
 ?
;
_chemical_name_common             ?
_chemical_melting_point           ?
_chemical_formula_moiety          ?
_chemical_formula_sum
 'Ag Bi51 Cu14 Pb52 S136'
_chemical_formula_weight          26789.45

loop_
 _atom_type_symbol
 _atom_type_description
 _atom_type_scat_dispersion_real
 _atom_type_scat_dispersion_imag
 _atom_type_scat_source
 'S'  'S'   0.1246   0.1234
 'International Tables Vol C Tables 4.2.6.8 and 6.1.1.4'
 'Cu'  'Cu'   0.3201   1.2651
 'International Tables Vol C Tables 4.2.6.8 and 6.1.1.4'
 'Ag'  'Ag'  -0.8971   1.1015
 'International Tables Vol C Tables 4.2.6.8 and 6.1.1.4'
 'Pb'  'Pb'  -3.3944  10.1111
 'International Tables Vol C Tables 4.2.6.8 and 6.1.1.4'
 'Bi'  'Bi'  -4.1077  10.2566
 'International Tables Vol C Tables 4.2.6.8 and 6.1.1.4'

_symmetry_cell_setting           'Monoclinic'
_symmetry_space_group_name_H-M   'C2/m  '

loop_
 _symmetry_equiv_pos_as_xyz
 'x, y, z'
 '-x, y, -z'
 'x+1/2, y+1/2, z'
 '-x+1/2, y+1/2, -z'
 '-x, -y, -z'
 'x, -y, z'
 '-x+1/2, -y+1/2, -z'
 'x+1/2, -y+1/2, z'

_cell_length_a                    37.432(8)
_cell_length_b                    4.0529(9)
_cell_length_c                    43.545(9)
_cell_angle_alpha                 90.00
_cell_angle_beta                  108.80
_cell_angle_gamma                 90.00
_cell_volume                      6254(2)
_cell_formula_units_Z             1
_cell_measurement_temperature     546(2)
```

```
_cell_measurement_reflns_used     ?
_cell_measurement_theta_min       ?
_cell_measurement_theta_max       ?

_exptl_crystal_description        ?
_exptl_crystal_colour             ?
_exptl_crystal_size_min          0.04
_exptl_crystal_size_mid          0.08
_exptl_crystal_size_max          0.15
_exptl_crystal_density_meas       ?
_exptl_crystal_density_diffrn     7.113
_exptl_crystal_density_method     'not measured'
_exptl_crystal_F_000              11126
_exptl_absorpt_coefficient_mu     72.953
_exptl_absorpt_correction_type   'empirical'
_exptl_absorpt_correction_T_min  0.0999
_exptl_absorpt_correction_T_max  0.7488
_exptl_absorpt_process_details    ?

_exptl_special_details
;
 ?
;

_diffrn_ambient_temperature       546(2)
_diffrn_radiation_wavelength      0.71073
_diffrn_radiation_type            MoK\a
_diffrn_radiation_source          'fine-focus sealed tube'
_diffrn_radiation_monochromator   graphite
_diffrn_measurement_device_type   ?
_diffrn_measurement_method        ?
_diffrn_detector_area_resol_mean  ?
_diffrn_standards_number          ?
_diffrn_standards_interval_count  ?
_diffrn_standards_interval_time   ?
_diffrn_standards_decay_%         ?
_diffrn_reflns_number             21473
_diffrn_reflns_av_R_equivalents   0.1124
_diffrn_reflns_av_sigmaI/netI     0.1040
_diffrn_reflns_limit_h_min        -50
_diffrn_reflns_limit_h_max        39
_diffrn_reflns_limit_k_min        -5
_diffrn_reflns_limit_k_max        5
_diffrn_reflns_limit_l_min        -57
_diffrn_reflns_limit_l_max        56
_diffrn_reflns_theta_min          1.39
_diffrn_reflns_theta_max          28.36
_reflns_number_total              8278
_reflns_number_gt                 6050
_reflns_threshold_expression      >2sigma(I)

_computing_data_collection        ?
_computing_cell_refinement        ?
_computing_data_reduction         ?
_computing_structure_solution     'SHELXS-97 (Sheldrick, 1990)'
```

```
_computing_structure_refinement   'SHELXL-97 (Sheldrick, 1997)'
_computing_molecular_graphics     ?
_computing_publication_material   ?

_refine_special_details
;
 Refinement of F^2^ against ALL reflections.  The weighted R-factor wR and
 goodness of fit S are based on F^2^, conventional R-factors R are based
 on F, with F set to zero for negative F^2^. The threshold expression of
 F^2^ > 2sigma(F^2^) is used only for calculating R-factors(gt) etc. and is
 not relevant to the choice of reflections for refinement.  R-factors based
 on F^2^ are statistically about twice as large as those based on F, and R-
 factors based on ALL data will be even larger.
;

_refine_ls_structure_factor_coef  Fsqd
_refine_ls_matrix_type            full
_refine_ls_weighting_scheme       calc
_refine_ls_weighting_details
 'calc w=1/[\s^2^(Fo^2^)+(0.0916P)^2^+361.7288P] where P=(Fo^2^+2Fc^2^)/3'
_atom_sites_solution_primary      direct
_atom_sites_solution_secondary    difmap
_atom_sites_solution_hydrogens    geom
_refine_ls_hydrogen_treatment     mixed
_refine_ls_extinction_method      SHELXL
_refine_ls_extinction_coef        0.000006(3)
_refine_ls_extinction_expression
 'Fc^*^=kFc[1+0.001xFc^2^\l^3^/sin(2\q)]^-1/4^'
_refine_ls_number_reflns          8278
_refine_ls_number_parameters      385
_refine_ls_number_restraints      0
_refine_ls_R_factor_all           0.1075
_refine_ls_R_factor_gt            0.0808
_refine_ls_wR_factor_ref          0.1957
_refine_ls_wR_factor_gt           0.1817
_refine_ls_goodness_of_fit_ref    1.062
_refine_ls_restrained_S_all       1.062
_refine_ls_shift/su_max           0.001
_refine_ls_shift/su_mean          0.000

loop_
 _atom_site_label
 _atom_site_type_symbol
 _atom_site_fract_x
 _atom_site_fract_y
 _atom_site_fract_z
 _atom_site_U_iso_or_equiv
 _atom_site_adp_type
 _atom_site_occupancy
 _atom_site_symmetry_multiplicity
 _atom_site_calc_flag
 _atom_site_refinement_flags
 _atom_site_disorder_assembly
 _atom_site_disorder_group
Bi1 Bi 0.09479(4) 0.0000 0.94994(3) 0.0155(3) Uani 1 2 d S . .
```

```
Bi2 Bi 0.43264(4) 0.0000 0.13679(3) 0.0167(3) Uani 1 2 d S . .
Pb3 Pb 0.31779(4) 0.0000 0.07426(3) 0.0176(3) Uani 1 2 d S . .
Pb4 Pb 0.20486(4) 0.0000 0.01401(3) 0.0172(3) Uani 1 2 d S . .
Pb5 Pb 0.04094(4) 0.0000 0.77609(3) 0.0173(3) Uani 1 2 d S . .
Pb6 Pb 0.15607(4) 0.0000 0.83874(3) 0.0167(3) Uani 1 2 d S . .
Pb7 Pb 0.27069(4) 0.0000 0.90086(4) 0.0184(3) Uani 1 2 d S . .
Bi8 Bi 0.48443(4) 0.0000 0.30993(3) 0.0146(3) Uani 1 2 d S . .
Pb9 Pb 0.37119(4) 0.0000 0.24780(3) 0.0167(3) Uani 1 2 d S . .
Bi10 Bi 0.25622(4) 0.0000 0.18681(4) 0.0184(3) Uani 1 2 d S . .
Bi11 Bi 0.09895(4) 0.0000 0.66333(4) 0.0187(3) Uani 1 2 d S . .
Bi12 Bi 0.21207(4) 0.0000 0.72516(3) 0.0157(3) Uani 1 2 d S . .
Bi13 Bi 0.40254(4) 0.0000 0.52779(3) 0.0156(3) Uani 1 2 d S . .
Pb14 Pb 0.29539(5) 0.0000 0.54228(4) 0.0215(3) Uani 1 2 d S . .
Bi15 Bi 0.18339(4) 0.0000 0.53685(3) 0.0154(3) Uani 1 2 d S . .
Bi16 Bi 0.08132(6) 0.0000 0.55147(5) 0.0183(7) Uani 0.764(16) 2 d SP . .
Ag Ag 0.08132(6) 0.0000 0.55147(5) 0.0183(7) Uani 0.236(16) 2 d SP . .
Bi17 Bi 0.37479(4) 0.0000 0.85603(4) 0.0193(3) Uani 1 2 d S . .
Pb18 Pb 0.33283(5) 0.0000 0.75041(4) 0.0231(3) Uani 1 2 d S . .
Bi19 Bi 0.31854(4) 0.0000 0.65074(4) 0.0179(3) Uani 1 2 d S . .
Bi20 Bi 0.02900(5) 0.0000 0.08667(4) 0.0249(4) Uani 1 2 d S . .
Bi21 Bi 0.06829(5) 0.0000 0.19275(4) 0.0205(3) Uani 1 2 d S . .
Pb22 Pb 0.07810(5) 0.0000 0.28961(4) 0.0277(4) Uani 1 2 d S . .
Pb23 Pb 0.10223(5) 0.0000 0.38832(4) 0.0223(3) Uani 1 2 d S . .
Pb24 Pb 0.38853(6) 0.0000 0.95691(5) 0.0371(5) Uani 1 2 d S . .
Pb25 Pb 0.00258(5) 0.0000 0.41319(5) 0.0349(5) Uani 1 2 d S . .
Pb26 Pb 0.31892(6) 0.0000 0.37196(5) 0.0337(4) Uani 1 2 d S . .
Cu Cu 0.5000 0.0000 0.5000 0.041(2) Uani 1 4 d S . .
Cu1 Cu 0.46890(16) 0.0000 0.01044(14) 0.0306(12) Uani 1 2 d S . .
Cu2 Cu 0.23127(16) 0.0000 0.30923(15) 0.0306(13) Uani 1 2 d S . .
Cu3 Cu 0.74933(15) 0.0000 0.58969(15) 0.0287(12) Uani 1 2 d S . .
S1 S 0.0649(3) 0.0000 -0.0044(2) 0.0140(18) Uani 1 2 d S . .
S2 S 0.4541(2) 0.0000 0.0831(2) 0.0136(18) Uani 1 2 d S . .
S3 S 0.3520(3) 0.0000 0.0180(3) 0.026(2) Uani 1 2 d S . .
S4 S 0.0203(3) 0.0000 0.8342(2) 0.0167(19) Uani 1 2 d S . .
S5 S 0.1281(3) 0.0000 0.8933(2) 0.019(2) Uani 1 2 d S . .
S6 S 0.2414(3) 0.0000 0.9573(2) 0.022(2) Uani 1 2 d S . .
S7 S 0.4916(3) 0.0000 0.7454(2) 0.021(2) Uani 1 2 d S . .
S8 S 0.3994(3) 0.0000 0.1925(2) 0.020(2) Uani 1 2 d S . .
S9 S 0.2873(3) 0.0000 0.1282(2) 0.020(2) Uani 1 2 d S . .
S10 S 0.1780(3) 0.0000 0.0649(3) 0.021(2) Uani 1 2 d S . .
S11 S 0.0310(3) 0.0000 0.3355(2) 0.0148(18) Uani 1 2 d S . .
S12 S 0.0729(3) 0.0000 0.7239(2) 0.020(2) Uani 1 2 d S . .
S13 S 0.1847(3) 0.0000 0.7847(2) 0.020(2) Uani 1 2 d S . .
S14 S 0.2911(3) 0.0000 0.8434(3) 0.027(2) Uani 1 2 d S . .
S15 S 0.4522(3) 0.0000 0.3607(2) 0.0150(18) Uani 1 2 d S . .
S16 S 0.3425(3) 0.0000 0.3066(2) 0.020(2) Uani 1 2 d S . .
S17 S 0.2381(3) 0.0000 0.2441(2) 0.0138(18) Uani 1 2 d S . .
S18 S 0.0520(3) 0.0000 0.4801(3) 0.020(2) Uani 1 2 d S . .
S19 S 0.1503(3) 0.0000 0.4615(2) 0.0134(18) Uani 1 2 d S . .
S20 S 0.2683(3) 0.0000 0.4733(2) 0.0148(18) Uani 1 2 d S . .
S21 S 0.3638(3) 0.0000 0.4538(3) 0.020(2) Uani 1 2 d S . .
S22 S 0.4679(3) 0.0000 0.4468(3) 0.023(2) Uani 1 2 d S . .
S23 S 0.1028(3) 0.0000 0.0957(2) 0.0158(18) Uani 1 2 d S . .
S24 S 0.1385(3) 0.0000 0.1930(2) 0.0173(19) Uani 1 2 d S . .
S25 S 0.1663(3) 0.0000 0.2964(2) 0.0156(18) Uani 1 2 d S . .
```

```
S26 S 0.1864(3) 0.0000 0.3930(2) 0.021(2) Uani 1 2 d S . .
S27 S 0.4714(3) 0.0000 0.9541(2) 0.019(2) Uani 1 2 d S . .
S28 S 0.4455(3) 0.0000 0.8570(2) 0.021(2) Uani 1 2 d S . .
S29 S 0.4075(3) 0.0000 0.7604(2) 0.0121(17) Uani 1 2 d S . .
S30 S 0.3906(3) 0.0000 0.6620(2) 0.0149(18) Uani 1 2 d S . .
S31 S 0.4404(3) 0.0000 0.5901(2) 0.0159(18) Uani 1 2 d S . .
S32 S 0.2229(3) 0.0000 0.5975(2) 0.0146(18) Uani 1 2 d S . .
S33 S 0.1236(4) 0.0000 0.6141(3) 0.028(2) Uani 1 2 d S . .
S34 S 0.2380(3) 0.0000 0.6769(2) 0.019(2) Uani 1 2 d S . .

loop_
 _atom_site_aniso_label
 _atom_site_aniso_U_11
 _atom_site_aniso_U_22
 _atom_site_aniso_U_33
 _atom_site_aniso_U_23
 _atom_site_aniso_U_13
 _atom_site_aniso_U_12
Bi1 0.0167(7) 0.0141(6) 0.0203(7) 0.000 0.0125(6) 0.000
Bi2 0.0180(8) 0.0149(6) 0.0213(7) 0.000 0.0122(6) 0.000
Pb3 0.0171(8) 0.0154(6) 0.0224(7) 0.000 0.0093(6) 0.000
Pb4 0.0182(8) 0.0148(6) 0.0211(7) 0.000 0.0100(6) 0.000
Pb5 0.0174(8) 0.0149(6) 0.0223(7) 0.000 0.0101(6) 0.000
Pb6 0.0176(7) 0.0151(6) 0.0208(7) 0.000 0.0112(6) 0.000
Pb7 0.0175(8) 0.0169(6) 0.0236(7) 0.000 0.0105(6) 0.000
Bi8 0.0114(7) 0.0131(6) 0.0209(7) 0.000 0.0075(6) 0.000
Pb9 0.0151(7) 0.0147(6) 0.0221(7) 0.000 0.0083(6) 0.000
Bi10 0.0173(8) 0.0164(6) 0.0238(7) 0.000 0.0100(6) 0.000
Bi11 0.0175(8) 0.0154(6) 0.0254(7) 0.000 0.0099(6) 0.000
Bi12 0.0160(7) 0.0154(6) 0.0211(7) 0.000 0.0136(6) 0.000
Bi13 0.0123(7) 0.0141(6) 0.0220(7) 0.000 0.0075(6) 0.000
Pb14 0.0210(8) 0.0188(7) 0.0272(7) 0.000 0.0114(7) 0.000
Bi15 0.0149(7) 0.0135(6) 0.0185(6) 0.000 0.0064(6) 0.000
Bi16 0.0181(12) 0.0157(10) 0.0271(12) 0.000 0.0155(9) 0.000
Ag 0.0181(12) 0.0157(10) 0.0271(12) 0.000 0.0155(9) 0.000
Bi17 0.0181(8) 0.0184(7) 0.0249(7) 0.000 0.0121(6) 0.000
Pb18 0.0240(9) 0.0163(7) 0.0301(8) 0.000 0.0104(7) 0.000
Bi19 0.0173(8) 0.0141(6) 0.0262(7) 0.000 0.0126(6) 0.000
Bi20 0.0266(9) 0.0182(7) 0.0280(8) 0.000 0.0060(7) 0.000
Bi21 0.0211(8) 0.0162(6) 0.0270(7) 0.000 0.0117(7) 0.000
Pb22 0.0346(10) 0.0205(7) 0.0282(8) 0.000 0.0106(8) 0.000
Pb23 0.0225(8) 0.0146(6) 0.0293(8) 0.000 0.0077(7) 0.000
Pb24 0.0375(11) 0.0327(9) 0.0350(9) 0.000 0.0031(9) 0.000
Pb25 0.0234(9) 0.0218(8) 0.0509(11) 0.000 0.0000(9) 0.000
Pb26 0.0299(10) 0.0327(9) 0.0459(10) 0.000 0.0224(9) 0.000
Cu 0.028(5) 0.067(6) 0.021(4) 0.000 -0.003(4) 0.000
Cu1 0.017(3) 0.035(3) 0.040(3) 0.000 0.011(3) 0.000
Cu2 0.018(3) 0.020(2) 0.058(4) 0.000 0.018(3) 0.000
Cu3 0.014(3) 0.023(2) 0.048(3) 0.000 0.008(3) 0.000
S1 0.022(5) 0.007(4) 0.022(4) 0.000 0.020(4) 0.000
S2 0.003(4) 0.017(4) 0.026(5) 0.000 0.011(4) 0.000
S3 0.035(7) 0.022(5) 0.025(5) 0.000 0.012(5) 0.000
S4 0.011(5) 0.024(5) 0.016(4) 0.000 0.005(4) 0.000
S5 0.022(5) 0.018(4) 0.019(4) 0.000 0.013(4) 0.000
S6 0.029(6) 0.013(4) 0.030(5) 0.000 0.016(5) 0.000
```

```
S7 0.015(5) 0.024(5) 0.028(5) 0.000 0.012(4) 0.000
S8 0.025(6) 0.017(4) 0.025(5) 0.000 0.018(5) 0.000
S9 0.027(6) 0.011(4) 0.029(5) 0.000 0.019(5) 0.000
S10 0.012(5) 0.017(4) 0.043(6) 0.000 0.021(5) 0.000
S11 0.009(4) 0.011(4) 0.023(4) 0.000 0.002(4) 0.000
S12 0.031(6) 0.017(4) 0.013(4) 0.000 0.007(4) 0.000
S13 0.038(6) 0.012(4) 0.017(4) 0.000 0.020(5) 0.000
S14 0.030(6) 0.016(5) 0.042(6) 0.000 0.019(5) 0.000
S15 0.011(4) 0.017(4) 0.017(4) 0.000 0.004(4) 0.000
S16 0.026(6) 0.018(4) 0.019(4) 0.000 0.013(4) 0.000
S17 0.008(4) 0.013(4) 0.023(4) 0.000 0.008(4) 0.000
S18 0.008(4) 0.012(4) 0.038(6) 0.000 0.004(4) 0.000
S19 0.010(4) 0.011(4) 0.020(4) 0.000 0.006(4) 0.000
S20 0.018(5) 0.009(4) 0.020(4) 0.000 0.010(4) 0.000
S21 0.006(4) 0.018(4) 0.042(6) 0.000 0.018(4) 0.000
S22 0.013(5) 0.022(5) 0.038(6) 0.000 0.014(5) 0.000
S23 0.016(5) 0.017(4) 0.018(4) 0.000 0.011(4) 0.000
S24 0.016(5) 0.015(4) 0.023(4) 0.000 0.007(4) 0.000
S25 0.006(4) 0.020(4) 0.024(4) 0.000 0.008(4) 0.000
S26 0.015(5) 0.022(5) 0.027(5) 0.000 0.010(4) 0.000
S27 0.018(5) 0.021(4) 0.019(4) 0.000 0.007(4) 0.000
S28 0.017(5) 0.031(5) 0.017(4) 0.000 0.010(4) 0.000
S29 0.013(4) 0.013(4) 0.016(4) 0.000 0.013(4) 0.000
S30 0.016(5) 0.011(4) 0.023(4) 0.000 0.013(4) 0.000
S31 0.012(5) 0.018(4) 0.022(4) 0.000 0.010(4) 0.000
S32 0.018(5) 0.010(4) 0.017(4) 0.000 0.008(4) 0.000
S33 0.038(7) 0.024(5) 0.030(5) 0.000 0.024(5) 0.000
S34 0.029(6) 0.013(4) 0.019(4) 0.000 0.013(4) 0.000

_geom_special_details
;
 All esds (except the esd in the dihedral angle between two l.s. planes)
 are estimated using the full covariance matrix.  The cell esds are taken
 into account individually in the estimation of esds in distances, angles
 and torsion angles; correlations between esds in cell parameters are only
 used when they are defined by crystal symmetry.  An approximate (isotropic)
 treatment of cell esds is used for estimating esds involving l.s. planes.
;

loop_
 _geom_bond_atom_site_label_1
 _geom_bond_atom_site_label_2
 _geom_bond_distance
 _geom_bond_site_symmetry_2
 _geom_bond_publ_flag
Bi1 S1 2.578(9) 1_556 ?
Bi1 S2 2.797(6) 7_546 ?
Bi1 S2 2.797(6) 7_556 ?
Bi1 S3 2.869(9) 7_556 ?
Bi1 S3 2.869(8) 7_546 ?
Bi1 S5 3.100(10) . ?
Bi2 S2 2.706(9) . ?
Bi2 S4 2.715(6) 7_556 ?
Bi2 S4 2.715(6) 7_546 ?
Bi2 S5 3.013(8) 7_546 ?
```